Available online at www.sciencedirect.com

SCIENCE DIRECT®

Geochimica et Cosmochimica Acta 70 (2006) 666–686

Geochimica

www.elsevier.com/locate/gca

Solid-state ^{13}C NMR analysis of size and density fractions of marine sediments: Insight into organic carbon sources and preservation mechanisms

Angela F. Dickens [a,b,*], Jeffrey A. Baldock [c], Ronald J. Smernik [d], Stuart G. Wakeham [e], Thórarinn S. Arnarson [a], Yves Gélinas [f], John I. Hedges [a,†]

[a] *School of Oceanography, University of Washington, Box 355351, Seattle, WA 98195-5351, USA*
[b] *Department of Chemistry, University of Washington, Box 351700, Seattle, WA 98195-1700, USA*
[c] *CSIRO Land and Water, PMB #2, Glen Osmond, SA 5064, Australia*
[d] *Soil and Land Systems, School of Earth and Environmental Sciences, The University of Adelaide, Waite Campus, Glen Osmond, SA 5064, Australia*
[e] *Skidaway Institute of Oceanography, 10 Ocean Sciences Circle, Savannah, GA 31411, USA*
[f] *Chemistry and Biochemistry Department, Concordia University, 1455, de Maisonneuve Blvd West, Montreal, Que., Canada H3G 1M8*

Received 4 October 2004; accepted in revised form 11 October 2005

Abstract

Burial of organic carbon (OC) in ocean sediments acts as the ultimate long-term sink for both terrestrial and marine carbon, however, the mechanisms controlling the preservation of this carbon are poorly understood. To better understand these mechanisms, we applied solid-state ^{13}C nuclear magnetic resonance (NMR) spectroscopy, along with elemental, stable carbon isotopic (δ^{13}C) and lignin phenol analyses, to size and density fractions of sediments influenced by either mixed terrestrial and marine OC inputs (Washington Coast slope) or dominantly marine inputs (Mexican Margin). Elemental, isotopic and lignin analyses all reveal that within the Washington Coast sediment, the OC mixes linearly between nitrogen-poor and ^{13}C-depleted, lignin-rich OC in the large and light fractions and nitrogen-rich and ^{13}C-enriched, lignin-poor OC in the small and dense fractions, suggesting that this sediment contains a two-component mixture of terrestrial vascular plant- and marine-derived OC. The integral areas of each of seven NMR spectral regions in the different samples trend linearly when plotted versus δ^{13}C signature, with most R^2 values of 0.78 or greater, demonstrating that the NMR spectra of the two sources of carbon also mix linearly between the two endmembers. The terrestrial endmember in this sediment appears to be dominated by lignin and black carbon whereas the source of the marine endmember is less clear from the NMR spectra. In contrast, all of the analyses indicate that OC in the Mexican Margin sediment fractions is homogenous and derives almost exclusively from marine sources. It appears that selective preservation of (bio)chemically recalcitrant lignin and black carbon is the primary mechanism of preservation of terrestrial OC, whereas mineral-protection is the dominant mechanism preserving marine OC in the Washington coast sediment. There is little evidence showing that either preservation mechanism functions in the Mexican Margin sediments.

1. Introduction

Burial of organic carbon (OC) in marine sediments is the ultimate long-term sink in the carbon cycle, removing the buried carbon from more rapidly cycling carbon pools for geologic time scales (Berner, 1989; Hedges and Keil, 1995). Burial of this OC also exerts an important control on atmospheric oxygen concentrations (Berner, 1989) and records a history of ocean processes through time (e.g., Prahl et al., 1988). However, most of the OC produced by primary production is degraded while cycling in the active carbon pools, and only a small fraction survives to be buried in sediments. Based on estimates of global marine net primary productivity and burial of OC in marine

---

[*] Corresponding author. Present address: Marine Chemistry and Geochemistry, MS#8, Woods Hole Oceanographic Institution, Woods Hole, MA 02543, USA.
E-mail address: adickens@whoi.edu (A.F. Dickens).

[†] Deceased.

0016-7037/$ - see front matter © 2005 Elsevier Inc. All rights reserved.
doi:10.1016/j.gca.2005.10.024

sediments ocean-wide (Berner, 1989), and assuming that all buried OC is from marine production, a maximum of around 0.4% of marine productivity may be preserved in sediments. However, this percentage is certainly an overestimate because significant amounts of terrestrial OC are also buried in ocean sediments. In fact, the terrestrial flux of OC to the oceans is large enough to account for all of the OC buried in the world's oceans (Ludwig et al., 1996; Hedges et al., 1997). Despite this, elemental and isotopic analyses show that most OC in marine sediments appears to derive from marine plankton, indicating that most of the terrestrially derived OC must be degraded in the oceans before burial in sediments (Hedges et al., 1997; Keil et al., 1997). However, a worldwide estimate of the efficiency of terrestrial OC preservation in marine sediments has proven elusive (Hedges et al., 1997).

Despite their importance in regulating OC burial, the mechanisms controlling the oxidation and preservation of sedimentary carbon remain poorly understood. Three primary mechanisms have been proposed to account for the preservation of OC in sediments and soils. (1) Humification, in which biopolymers break down into individual monomers which then abiotically polymerize to form amorphous, humic materials (Stevenson, 1994), is the traditional explanation. However, many lines of evidence, from both nuclear magnetic resonance (NMR) spectroscopy (e.g., Knicker, 2000; Hedges et al., 2001) and molecular-level analyses (e.g., Hatcher et al., 1983) suggest that this mechanism does not dominate in the environment (Hedges et al., 2000a; Burdon, 2001). (2) Selective preservation of biomolecules resistant to degradation appears to play a role in preserving OC in both soils and sediments (Hatcher et al., 1983; Derenne et al., 1991; Hwang and Druffel, 2003). In reality, this mechanism represents selective degradation of labile molecules, leading to enrichment of resistant biochemicals such as lignin, peptidoglycan and algaenans, along with black carbon (i.e., charcoal) derived from combustion (Hedges et al., 2000a; Derenne and Largeau, 2001). (3) Finally, physical protection of OC via association with minerals or encapsulation in resistant organic structures has been proposed as a mechanism for preserving OC (Keil et al., 1994a; Knicker and Hatcher, 1997; Arnarson and Keil, 2005). Evidence for this mechanism derives primarily from the relatively constant relationship between %OC and mineral surface area in sediments worldwide (Mayer, 1994; Keil and Cowie, 1999) and from an observed lack of selectivity during degradation of OC in sinking particles in several environments (Hedges et al., 2001; Minor et al., 2003).

It has proven difficult to test the importance of these different mechanisms in protecting OC from degradation in part because the OC itself is very difficult to characterize. During the conversion of fresh biomass to degraded material, the percent of molecularly recognizable carbon decreases dramatically (Hedges et al., 2000a), declining from, for example, around 80% in plankton of the Equatorial Pacific to about 20% in the underlying sediments (Wakeham et al., 1997). Other commonly applied approaches in the field (i.e., elemental and isotopic analyses) provide very broad information about the average OC in the sample, but yield little detail about the structure of the OC and the processes affecting this OC.

Nuclear magnetic resonance spectroscopy is an excellent tool for determining the mechanisms by which OC is preserved in the ocean. NMR spectroscopy provides information about the functional group distribution of all of the OC in a sample, providing a basis for inferring the molecular structure of the total OC (i.e., Nelson et al., 1999; Preston et al., 1990; Baldock et al., 2004). NMR observabilities are not affected by degradation, and with careful attention to experimental setup, NMR spectra can be acquired quantitatively (Kinchesh et al., 1995; Smernik and Oades, 2000a,b, 2003). NMR spectroscopy has been applied extensively to study soil organic matter (as reviewed in Preston, 1996; Kögel-Knabner, 1997) but remains underutilized in studies of marine systems (e.g., Gélinas et al., 2001a, Hedges et al., 2001, 2002; Golding et al., 2004).

Physical fractionation of sediments is another useful tool for determining how OC is preserved in sediments, and particularly for determining the importance of mineral association in protecting OC, because it allows separation of OC according to its association with different minerals. Density fractionation separates sediments according to the degree of mineral association, with light fractions containing mostly OC and dense fractions mostly minerals (Bock and Mayer, 2000; Arnarson and Keil, 2001). Fractionation according to size separates OC associated with different sizes of mineral particles or differently sized, discreet OC particles (Christensen, 1992; Keil et al., 1994b).

We applied solid-state ^{13}C NMR spectroscopy to size and density fractions of two sediments in order to characterize the OC and its physical associations and to infer the mechanisms allowing the preservation of that OC. In addition to NMR analysis, we analyzed the elemental (carbon and nitrogen) and stable carbon isotopic (δ^{13}C) composition of the sediment fractions. These analyses, in combination with quantification of lignin biomarkers, allow a better understanding of the processes affecting the sedimentary OC. We studied one sediment from the Washington Coast slope which contains a mixture of terrestrial and marine inputs (Hedges and Mann, 1979) as well as a sediment from the anoxic region off the western Mexican Margin which contains almost entirely marine OC (Ganeshram et al., 1999). By comparing these two sites, we aimed to better understand the fates and preservation mechanisms of terrestrial and marine OC in the oceans.

2. Materials and methods

2.1. Study locations and samples

The Washington Margin has a relatively narrow continental shelf cut by marine canyons, and sediments along this margin are dominated by inputs from the Columbia

River (White, 1970; Nittrouer and Sternberg, 1981). Riverine sediments that are initially deposited on the shelf near the river mouth are resuspended and carried northward during winter storms, and finer clays and silts are carried offshore to the continental slope and Cascadia Basin (Nittrouer and Sternberg, 1981; Hedges et al., 1999). Sediments may undergo repeated deposition and resuspension cycles ("hop-scotch") as they are transported offshore, taking from <1 to 70 years to reach the continental slope (Keil et al., 2004). The sediments are mostly lithogenic (continental), containing a mixture of clay minerals, quartz, feldspar and mica, with very little $CaCO_3$ and <15% opal (Keil et al., 1994b). OC along this margin derives from both terrigenous and marine sources, with a decreasing terrestrial contribution away from the shore (Hedges and Mann, 1979; Prahl et al., 1994).

Sediment sources and transport along the Mexican Margin are less well-understood. The continental shelf on this margin is narrow, and sediments are primarily lithogenic, with smaller amounts of biogenic sediments (Van Andel, 1964). Intense winnowing of shelf sediments transports fine-grained sediments to the slope, and calcareous clayey silts on the outer shelf and upper slope grade into silty clays farther offshore (Van Andel, 1964; Ganeshram et al., 1999). There is a strong oxygen-deficient zone (ODZ) between ~100 and 1000 m (Hartnett et al., 1998; Hartnett and Devol, 2003), in which sediments are characterized by high OC concentrations (6–10%) and no bioturbation (Ganeshram et al., 1999; Hartnett and Devol, 2003). Sediments within the ODZ contain a mixture of clay minerals, quartz and feldspars, with significant amounts of biogenic opal and $CaCO_3$ (Van Andel, 1964; Arnarson and Keil, 2001). OC along this margin derives dominantly from marine sources (Ganeshram et al., 1999).

The Washington Coast Slope sediment was collected using a multicorer from the R/V *New Horizon* in 2001. This location (46° 49.0′ N, 125° 00.4′ W) is within the oxygen minimum zone and has a water depth of 640 m. Sediments were sectioned into 1-cm intervals and transported frozen back to the lab. The top 6 cm were pooled to provide the composite surface sample used in this study. The Mexican Margin sediment was collected using a Soutar box core from the R/V *New Horizon* in 1996. The sediment was subsampled using a 7.5 cm-diameter core tube and sectioned into 5-cm intervals. This sample is from the top 5 cm of core NH96-204 (22° 41.78′ N, 106° 28.61′ W) from within the suboxic zone at a water depth of 395 m.

We obtained a culture of the gram-negative marine sedimentary bacteria *Vibrio mediterranei* (43.8% C; 11.8% N; 8.9% H) from the American Type Culture Collection (ATCC #43341) and cultured the organisms in Bacto Marine Broth Difco 2216 media. Samples were grown in the dark at room temperature until reaching the stationary stage of growth (~24 h), at which point the cells were isolated by centrifuging the media at 6300 rpm for 5 min and decanting the supernatant. The isolated cells were rinsed with deionized water 3 times and freeze-dried. The charcoal sample (69.2% C; 1.8% N) was made from mesquite wood charred in a kiln with limited air circulation, and the lignin sample (61.9% C; 5.9% H) is an alkali lignin from Sigma Chemicals.

2.2. Density and size fractionation

Sediments were density fractionated as described in Dickens et al. (2004) using heavy liquid flotation in sodium polytungstate solutions at densities of 1.6, 2.0 and 2.5 g/cm^3 (Arnarson and Keil, 2001). After centrifugation, the floating particles were transferred to a different tube and the procedure was repeated until no additional floating material was observed, which required as many as 41 iterations. We then added the next heaviest solution and repeated the procedure for the remaining density fractions. Samples were rinsed with deionized water and freeze-dried.

The size fractionation technique is also described in Dickens et al. (2004). Briefly, sediments were sieved through 250, 63 and 38 μm stainless steel sieves, and the <38 μm fraction was separated using SPLITT-fractionation, a form of field flow fractionation, into hydrodynamic classes corresponding to nominal cutoffs of ~17 and 3 μm (Giddings, 1985; Keil et al., 1994b). Before separation, sediments were sonicated using a sonic probe in order to disrupt aggregates of smaller particles that could interfere with accurate hydrodynamic sorting (Ransom et al., 1998; Bock and Mayer, 2000). In order to minimize inclusion of smaller sized particles in the larger fractions, after each separation step the larger fraction was sonicated again and rerun through the same separation. Collected fractions were recovered via centrifugation and freeze-dried. Very fine particles (nominally <1 μm) that remained in the carrier solution after centrifugation were flocculated by addition of sodium chloride to create a 10‰ solution.

2.3. Chemical analyses

Weight percent organic carbon and nitrogen and stable carbon isotopes were determined after acidification using the method outlined in Ward et al. (2001). Analyses were performed by elemental analyzer—continuous flow isotope ratio mass spectrometry (EA/CFIRMS), using a Carlo Erba NC2500 interfaced through a Finnigan CONFLO II to a Finnegan Delta XL mass spectrometer. All isotope ratios are expressed in δ notation, or parts per thousand deviation from the Vienna PeeDee Belemnite (VPDB) standard, where:

$$\delta^{13}C = \{[(^{13}C/^{12}C)_{sample}/(^{13}C/^{12}C)_{VPDB}] - 1\} * 1000.$$

For those samples which did not have enough OC for isotopic analysis, weight percent organic carbon and nitrogen was measured after acidification with a Carlo Erba model 1106 CHN analyzer (Hedges and Stern, 1984).

Lignin phenols were quantified by the cupric oxide oxidation method of Hedges and Ertel (1982) as modified by

Goñi and Hedges (1992). Samples containing approximately 5 mg OC were ground and oxidized at 155 °C (internal reactor temperature) for 3 h with CuO under basic (8% NaOH) conditions. Reaction products were acidified, extracted with ethyl ether, dried and converted to trimethylsilyl (TMS) counterparts. TMS derivatives were analyzed with an average precision of ±10% using a Hewlett–Packard 5890 gas chromatograph fitted with a flame ionization detector and a fused silica capillary column coated with DB1 liquid phase. Lignin phenols were quantified based on the recoveries of ethyl-vanillin, and individual response factors were derived from periodically injected mixtures of commercial standards.

2.4. Demineralization

To remove paramagnetic cations that would interfere with NMR analysis and to concentrate OC, sediment fractions were demineralized in preparation for NMR analysis according to the method detailed in Gélinas et al. (2001b). Minerals were dissolved by sequential treatments with 1 N HCl followed by two treatments with 1 N HCl/10% HF. OC losses during the treatment ranged from 0% to 13% for the Washington Coast sediments and from 0% to 21% for most of the Mexican Margin sediments, small enough losses that OC was not recovered from the supernatant solutions. However, the Mexican Margin 17–63 and >63 μm fractions lost 52.0% and 79.6% of their carbon. The large losses observed in the last two samples indicate that the NMR spectra for these samples are probably not representative of the total OC in these fractions, but this lost OC represents only a small component (~5%) of the total OC in the Mexican Margin sediment. Overall, between 5% (for the summed Washington Coast size fractions) and 13% (for the summed Mexican Margin density fractions) of the total OC in the fractions was lost during demineralization.

2.5. NMR analysis

Solid state ^{13}C NMR spectra were obtained at a ^{13}C frequency of 50.3 MHz on a Varian Unity200 spectrometer. Samples of known mass (10–130 mg OC) were packed in a 7 mm diameter cylindrical zirconia rotor with Kel-F end caps and spun at the magic angle at a rate of 5000 ± 100 Hz in a Doty Scientific MAS probe. Free induction decays were acquired with a sweep width of 40 kHz; 1216 data points were collected over an acquisition time of 15 ms. All spectra were zero filled to 8192 data points and processed with a 50-Hz Lorentzian line broadening and a 0.010 s Gaussian broadening. Chemical shifts were externally referenced to the methyl resonance of hexamethylbenzene at 17.36 ppm. After linear baseline correction between 300 and −100 ppm, spectral distributions for all samples were determined by integrating signal intensities within each of the eight chemical shift regions given in Table 4. The chemical shift boundaries of these regions were selected based on previous experience with quantification of ^{13}C NMR spectral data (e.g., Skjemstad et al., 1999; Hedges et al., 2002). Areas were divided into individual spectral regions by dropping vertical lines to a baseline defined by the Varian VNMR operating software between 300 and −10 ppm.

Cross-polarization (CP) spectra were acquired using a standard CP pulse sequence and magic angle spinning (Wilson, 1987) with a 1.0-ms contact time and a recycle delay of 500 ms, a length of time >7 times the average T_1H value (proton spin lattice relaxation rate constant—see below) for each sample. Either 10,000 or 100,000 transients were collected for each spectrum, depending on the amount of carbon in the rotor. Signal intensities associated with spinning side bands of all major resonances above 110 ppm were numerically allocated back to the spectral region from which they were derived (Baldock and Smernik, 2002). Triplicate CP/MAS ^{13}C NMR analyses were made for both of the unfractionated, bulk samples by repacking aliquots of the same material into a rotor and acquiring spectra under otherwise identical conditions. The overall reproducibility with which major areas (>2% of total spectral area) could be determined by triplicate analyses of individual spectral regions averaged ±2% (percent sample mean deviation) of the measured value.

Bloch decay (BD) spectra were acquired using a 6.2 μs (90°) ^{13}C pulse and a recycle delay of 90 s, and 1000 transients were collected for each sample. All BD spectra were corrected for background signal according to Smernik and Oades (2001).

The fraction of OC in the samples that was observed by NMR (C_{obs}) was assessed for all CP and BD spectra using the spin counting method of Smernik and Oades (2000a,b) with glycine as the external standard and NMR conditions optimized separately for glycine and the samples. $C_{obs} - CP$ and $C_{obs} - BD$ values were determined according to Eqs. (1) and (2), respectively. Errors are estimated to be ±10% in $C_{obs} - CP$ and ±15% in $C_{obs} - BD$ (Smernik and Oades, 2000a).

$$C_{obs} - CP = \left(\frac{\left(\frac{\text{Sample } T_{1\rho}\text{H}-\text{corrected signal intensity}}{\text{Mass of sample C analyzed(mg)}} \right)}{\left(\frac{\text{Glycine } T_{1\rho}\text{H}-\text{corrected signal intensity}}{\text{Mass of glycine C analyzed(mg)}} \right)} \right), \quad (1)$$

$$C_{obs} - BD = \left(\frac{\left(\frac{\text{Sample BD signal intensity}}{\text{Mass of sample C analyzed(mg)}} \right)}{\left(\frac{\text{Glycine BD signal intensity}}{\text{Mass of glycine C analyzed(mg)}} \right)} \right). \quad (2)$$

2.5.1. RESTORE, $T_{1\rho}H$ and T_1H

To determine which types of OC were underrepresented in the CP spectra, a subset of the samples were analyzed using five different NMR experiments: one variable contact time (VCT) experiment, three variable spin lock (VSL) experiments, and one RESTORE experiment (Smernik and Oades, 2003). Rates of proton spin-lattice relaxation in the static frame ($1/T_1H$) were determined using the methodology of Smernik et al. (2000) involving an inversion-recovery pulse sequence. Rates of proton spin-lattice relaxation in the rotating frame ($1/T_{1\rho}H$) were determined using a 1-ms contact time VSL pulse sequence (Alla and Lippmaa, 1976). Values of $T_{1\rho}H$ were calculated as the inverse slope of the graph of ln(total signal intensity) versus spin lock time.

2.5.2. *Proton spin relaxation editing*

Proton spin relaxation editing (PSRE) was used to generate subspectra of the rapidly and slowly relaxing components identified in inversion recovery experiments using the method of Smernik et al. (2000). PSRE involves taking linear combinations of a "normal" CP spectrum and a partially relaxed inversion recovery spectrum to generate "pure" subspectra of the rapidly relaxing and slowly relaxing components. The recovery delay for the partially relaxed spectrum was chosen to minimize noise in the subspectra (Smernik et al., 2000).

2.5.3. *Molecular mixing model*

The distribution of four biochemicals (lignin, protein, carbohydrate and lipid) and charcoal present in a sample were estimated using a molecular mixing model (Nelson et al., 1999; Hedges et al., 2002; Baldock et al., 2004). Average CP NMR spectral characteristics were calculated for each of these five nominal endmembers based on literature values for the relative abundances and carbon functionalities of their chromatographically resolved structural units (e.g., amino acids) or based on spectra of representative samples (e.g., pine charcoal). The five endmembers were then numerically mixed in the model to determine the percentage of each biochemical that gave the best overall agreement between the calculated and measured CP spectral abundances of the sample.

3. Results and discussion

3.1. *Mass, organic carbon and nitrogen yields and distribution*

We fractionated the two sediments according to both the density and size of individual particles in order to investigate the mineral associations and chemical composition of the OC in the two environments being studied. We separated sediments into four density fractions, (<1.6, 1.6–2.0, 2.0–2.5 and >2.5 g/cm^3), with increasing density generally corresponding to decreasing loading of relatively light OC onto dense sedimentary minerals (Table 1). We also fractionated sediments into five size fractions corresponding to clays (<1 and <3 μm), fine and coarse silts (3–17

Table 1
Mass, elemental, isotopic and lignin yields and properties from physical fractions of sediments

Sample	Symbol	% Recovery			wt %	OC conc.[a] (%)	$(N:C)_a$[a]	$\delta^{13}C$ (‰)	Λ[a] (mg/100 mg OC)	$(Ad/Al)_v$[a]	%terr.[a]
		Mass	OC[a]	N[a]							
Washington Slope											
Bulk	B					2.47	0.100	−21.8	0.93	0.38	21
Density fractions		90.1	69.1	82.7							
>2.5 g/cm^3	d				43.8	0.10	0.210	−22.0	n.d.	n.d.	n.d.
2.0–2.5 g/cm^3	h				43.7	2.64	0.123	−21.0	0.45	0.48	6
1.6–2.0 g/cm^3	m				11.4	6.06	0.112	−21.8	0.75	0.36	23
<1.6 g/cm^3	l				1.1	33.78	0.050	−24.6	3.60	0.30	78
Size fractions		93.0	65.4	72.1							
<1 μm	sc				7.5	6.84	0.119	−21.3	0.76	0.46	12
<3 μm	mc				19.0	2.62	0.113	−22.1	1.19	0.37	28
3–17 μm	ss				39.8	2.30	0.108	−22.4	1.30	0.33	35
17–63 μm	ms				29.0	0.37	0.090	−23.3	1.93	0.27	52
>63 μm	sa				4.5	0.81	0.067	−23.2	2.82	0.40	49
Mexican Margin											
Bulk						7.19	0.096	−20.1			
Density fractions		n.d.[a]	n.d.[a]	n.d.[a]							
>2.5 g/cm^3					8.8	0.34	0.106	n.d.			
2.0–2.5 g/cm^3					27.8	2.24	0.118	−20.1			
1.6–2.0 g/cm^3					57.7	8.75	0.104	−20.0			
<1.6 g/cm^3					6.4	28.87	0.090	−20.4			
Size fractions		83.7	69.5	67.5							
<1 μm					2.6	17.42	0.096	−20.8			
<3 μm					55.0	7.63	0.100	−20.7			
3–17 μm					32.9	4.43	0.099	−20.6			
17–63 μm					9.1	1.90	0.140	−21.3			
>63 μm					0.4	36.78	0.154	−20.1			

[a] OC, organic carbon; N, nitrogen; wt%, weight percent; $(N:C)_a$, atomic nitrogen-to-carbon ratio; Λ, the sum of 8 lignin phenols; $(Ad/Al)_v$, the acid-to-aldehyde ratio of vanillyl phenols; %terr, % terrestrial OC, calculated as described in the text using the method of Prahl et al. (1994). n.d., not determined.

and 17–63 μm) and sands (>63 μm). Both fractionation methods were optimized to obtain samples that were as representative as possible of the nominal size or density fraction and free of contamination by materials from other fractions, but the additional processing probably also led to increased sample losses during fractionation.

During density fractionation, we recovered 90.1% of the Washington Coast sediment (Table 1). We could not calculate the recovery of the Mexican Margin sediment because the initial sediment mass was not measured. The Washington Coast sediment was dominated by the two densest fractions, which combined to account for a total of 87.5% of the total recovered mass (Table 1, Fig. 1A). In contrast, only 36.6% of the Mexican Margin sediment fell into the densest two fractions, whereas 57.7% was in the 1.6–2.0 g/cm^3 fraction. We recovered less OC (69.1%) and nitrogen (82.7%) than mass from the Washington Coast sediment (Table 1). Our mass recovery was somewhat better than that of Arnarson and Keil (2001), but our OC and N recoveries were poorer, perhaps due to larger losses of the OC-rich light fraction during the 41 iterations required for its isolation. The OC was most concentrated in the light fractions of both sediments and decreased as density increased (Table 1). For the Washington Coast sample, over 55% of the OC was found in the 2.0–2.5 g/cm^3 fraction, with the yield of OC decreasing at lower densities and very little OC found in the densest fraction (Fig. 1C). This indicates that most OC in the Washington Coast sediment is closely associated with minerals, probably as organo-clay complexes (Bock and Mayer, 2000). Nitrogen follows a similar distribution but is more enriched in the heavier fractions and depleted in the light (Fig. 1C). More than 65% of the recovered Mexican Margin OC fell into the 1.6–2.0 g/cm^3 fraction, with another 23.8% in the light fraction and smaller amounts in the densest fractions (Fig. 1C), demonstrating that OC in this sediment is less closely associated with sedimentary minerals than in the Washington Coast sediment. Nitrogen tracks OC almost perfectly in this sediment, suggesting chemical homogeneity of the OC (Fig. 1C).

Percent mass recoveries from size fractionation were 93.0% for the Washington Coast sample and 83.7% for the Mexican Margin sediment (Table 1). Most of the Washington Coast sediment was found in the fine and coarse silt fractions, with these two fractions containing 39.8% and 29.0% of the total recovered mass, respectively (Table 1; Fig. 1B). The Mexican Margin sample was dominated by clays, with over 55.0% of the mass in the <3 μm fraction (Table 1). We recovered 65.4% and 69.5% of the OC and 72.1% and 67.5% of the N from the Washington and Mexican sediments, respectively. Our mass, OC and N recoveries are lower than those of Keil et al. (1994b), probably because we ran each fraction through the fractionation twice in order to isolate fractions that were as pure as possible. For the Washington Coast sample, the OC was most concentrated in the smallest size fractions and decreased as size increased (Table 1). The Mexican Margin sediment had high %OC in both the smallest and largest size fractions, with the lowest concentration in the 17–63 μm fraction. Most of the OC in the Washington Coast sample was divided between the clay and fine silt fractions, with 23–24% of the OC in each of the two smallest size fractions and another 43.0% in the fine silt fraction (Fig. 1D). Nitrogen followed a similar pattern (Fig. 1D). This reinforces the interpretation of the density data suggesting that OC in this sediment is closely associated with fine sedimentary minerals. In the Mexican Margin sample, over 55% of the OC and N sorted into the <3 μm clay fraction (Fig. 1D). Combined with the density data, this sug-

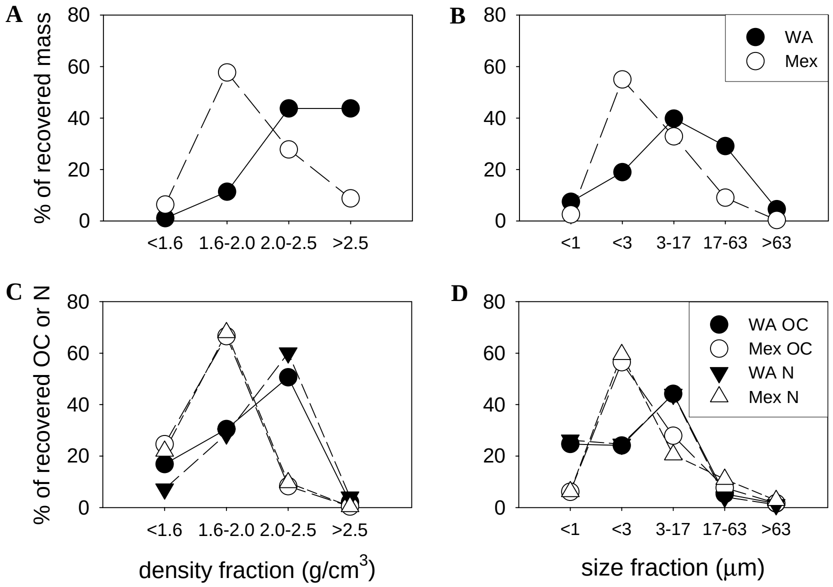

Fig. 1. Mass (top), organic carbon (OC) and nitrogen (N) (bottom) distribution in density (left) and size (right) fractions of Washington Coast (filled symbols) and Mexican Margin (open symbols) sediments.

gests that most of the OC in the Mexican Margin is associated with clay minerals.

3.2. Elemental ratios, stable carbon isotopic signatures and lignin yields

For the Washington Coast sediment, the N/C ratios ranged between 0.050 and 0.210, with the smallest values in the lightest and largest fractions and the largest values in the heavy and small fractions (Table 1). The extremely high value observed in the densest fraction may be due to preferential sorption of N-rich amino acids (Aufdenkampe et al., 2001) or to sorption of inorganic nitrogen onto these OC-poor minerals (Hedges et al., 2000b). Because it contains such a small fraction (2%) of the OC and appears to derive from different sources than the bulk OC, we did not consider this sample in further analyses. The Mexican Margin OC had fairly homogenous N/C ratios ranging from 0.090 to 0.154 and showed no clear trends with size or density, although the light fraction was the most depleted of nitrogen, as was the case for the Washington Coast sediment (Table 1). The $\delta^{13}C$ values for the Washington Coast sample ranged from around −21‰ for the dense and small fractions up to −24.6‰ for the lightest fraction, and the Mexican Margin samples had very homogeneous $\delta^{13}C$ values around −20‰ (Table 1).

Fig. 2A shows that the Washington Coast samples contain a mixture of marine plankton and C_3 terrestrial OC, as illustrated by the linearity ($R^2 = 0.86$) of the plot of N/C versus $\delta^{13}C$ for these fractions. The small and dense fractions resemble marine plankton both elementally and isotopically, whereas the large and light samples appear to contain large amounts of terrestrially derived C_3 vascular plant material. OC derived from C_4 plants does not appear to be important. The linearity of the plot suggests that OC in the sediments from this site is a two-component mixture of marine and relatively unaltered C_3 plant debris, containing little mineral-associated soil-derived OC (hereafter described as "soil OC"). Keil et al. (1994b) found similar linear relationships for the OC in size fractions of other Washington Coast sediments, although they found evidence of significant amounts of soil OC in the clay-sized fractions. Based on Fig. 2, it is possible that our small and dense fractions contain small amounts of soil OC, rather than vascular plant OC, but it remains clear that most of the terrestrial OC in this Washington Coast sediment derives from vascular plant debris.

We also analyzed our sediment fractions for the amount of lignin, a structural component of vascular plants that is often used as a tracer of terrestrial OC in the ocean (Hedges and Mann, 1979). For the Washington Coast, the highest yields of lignin phenols were from the large and light fractions, up to 3.60 mg total lignin phenols/100 mg OC (Λ) in the light fraction, and the least from the small and dense fractions, with the smallest yield (0.45/100 mg OC) from the densest measurable fraction (Table 1). Fig. 2B shows that Λ trends linearly with $\delta^{13}C$ signature ($R^2 = 0.91$), with the most lignin in the most terrestrial (^{13}C-depleted) samples. Λ is even more strongly correlated to the elemental N/C ratio ($R^2 = 0.95$, not shown). The linearity of these relationships between different markers of terrestrial versus marine OC in our sediment fractions further enforces the proposition that our Washington Coast sediment fractions contain a mixture of terrestrial and marine OC. Vanillyl phenols were the most abundant lignin oxidation products (Table A1), and a plot of the ratio of syringyl to vanillyl phenols (S/V) versus that of cinnamyl to vanillyl phenols (C/V; not shown) indicated that the lignin derived from a mixture of woody and non-woody gymnosperm material, as was found previously for sediment from this environment (Keil et al., 1998). However, these parameters did not trend with density or size. The acid to aldehyde ratio (Ad/Al) of lignin phenols has been used as an indicator of the degree of oxidation of lignin in sedi-

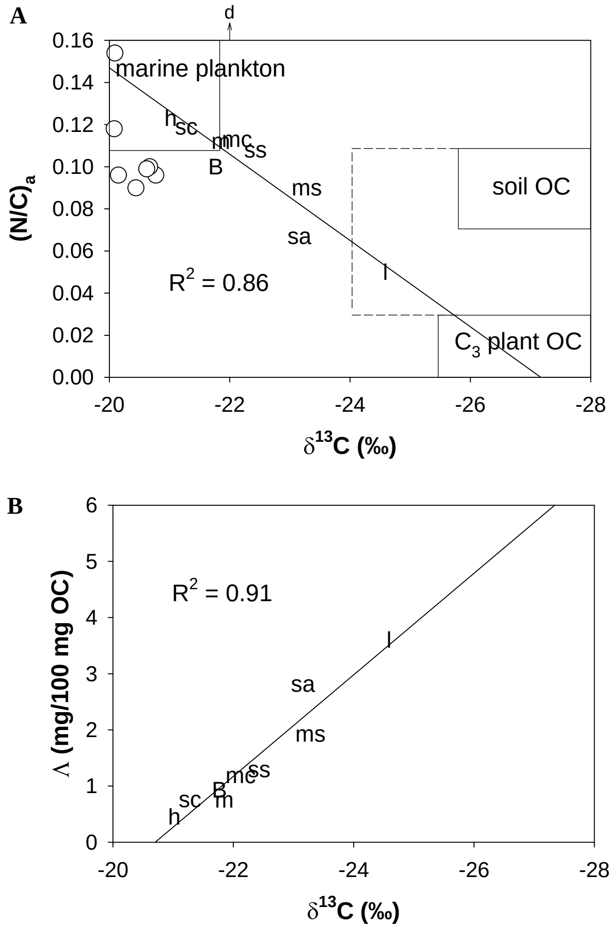

Fig. 2. Elemental, isotopic and lignin yields of Washington Coast sediment fractions. (A) Atomic nitrogen:carbon ratios plotted versus stable carbon isotopic signature. Boxes shown outline typically observed ranges within the Columbia River watershed for possible sources of carbon to the sediments (Keil et al., 1994b). The dotted extension of the soil OC box represents the isotopic range for soil OC observed in soils worldwide (derived from C_3 vegetation). C_4 vegetation and soil lie off the plot, with similar N/C ratios to C_3 material but $\delta^{13}C$ values of −12 to −16‰. Symbols for Washington slope sediment fractions are as listed in Table 1. Mexican Margin fractions are shown for reference as open circles. (B) Lignin yield (Λ) plotted versus stable carbon isotopic signature.

ments (Goñi et al., 1993). We found that this ratio was generally highest in the smallest and densest fractions, indicating that these fractions had experienced the greatest degree of oxidation, although the largest size fraction also had a high ratio (Table 1). It is possible, and could be consistent with slight deviations in these fractions from the linear fit in the N/C versus $\delta^{13}C$ plot (Fig. 2A), that these small amounts of highly degraded lignin in the small and dense fractions derived from OC that became sorbed to soil minerals and underwent degradation in soils, as concluded by Keil et al. (1998). We did not analyze the Mexican Margin sediments for lignin.

We estimated the percent of terrestrially derived OC (%terr) in the Washington Coast sediment based on the combined lignin biomarker and isotopic approach of Prahl et al. (1994) using Eq. (3):

$$\%\mathrm{terr} = \frac{(\delta^{13}C_{\mathrm{sediment}} - \delta^{13}C_{\mathrm{marine}})}{(\delta^{13}C_{\mathrm{terrestrial}} - \delta^{13}C_{\mathrm{marine}})} \times 100, \tag{3}$$

where $\delta^{13}C_{\mathrm{terrestrial}}$ and $\delta^{13}C_{\mathrm{marine}}$ are estimated isotopic signatures for the two endmembers. $\delta^{13}C_{\mathrm{marine}}$ is derived from extrapolating the regression shown in Fig. 2B to $\Lambda = 0$ ($\delta^{13}C = -20.7‰$), and $\delta^{13}C_{\mathrm{terrestrial}}$ is estimated to be $-25.7‰$ based on measurements of terrestrial material delivered to the Washington Margin from the Columbia River (Prahl et al., 1994). We performed these calculations using the isotopic relationship rather than the more highly correlated elemental ratio relationship because constraining the N/C ratio of terrestrial endmembers has proven problematic and yielded impossible results (Prahl et al., 1994). We estimated that the bulk Washington Coast sediment contains 21% terrestrial OC, intermediate between previous estimates for this region (Prahl et al., 1994; Keil et al., 1994b; Keil et al., 2004). The sediment fractions contain between 6% and 78% terrestrial OC, with the smallest percentages in the densest and smallest size fractions and the greatest percentages in the lightest and largest size fractions (Table 1). This trend agrees with the elemental and lignin phenol trends discussed above.

3.3. Comparison of CP, BD and RESTORE ^{13}*C NMR spectra*

We used two different polarization techniques to acquire NMR spectra: Bloch decay (BD) and cross polarization (CP). Bloch decay, in which the ^{13}C nuclei are directly irradiated, is the more quantitative of the techniques. However, it is also produces approximately 4 times less signal per scan and requires delays between scans (recycle delays) that are about 100 times longer than are required for CP, leading to poorer signal-to-noise ratios and longer acquisition times. With CP, the ^{1}H nuclei are irradiated and then transfer magnetization to the ^{13}C nuclei. This makes CP less quantitative than BD due to decreased signal from ^{13}C nuclei that are far from their nearest neighbor ^{1}H (i.e., condensed aromatic structures like charcoal) or linked to ^{1}H nuclei that relax rapidly during the magnetization transfer. It is generally not practical to analyze all samples using BD, and CP is the most commonly used technique, however, it is important to understand how representative CP spectra are of total carbon in a sample.

Spin counting is a technique that determines the percent of OC in a sample that is observed by NMR (the observability, C_{obs}; Smernik and Oades, 2000a,b) by comparing the amount of NMR signal observed from a sample with the amount of signal expected if all of the carbon in the sample were observed. Low observabilities indicate that a spectrum may not be representative of the total OC in a sample, depending on whether the signal loss is selective or non-selective. Table 2 shows the observabilities for both our CP and BD spectra. Three samples did not contain enough OC to allow collection of a CP spectrum, and several more contained too little for a BD spectrum. C_{obs} for our CP spectra ranged between 35% and 85%, with an average of 65%. Only one sample had an observability of less than 50%, perhaps because of incomplete removal of paramagnetics during demineralization. (Because this sample had an order of magnitude lower %OC than any other sample analyzed by NMR, we were not able to concentrate its OC as well as for other samples.) C_{obs} was higher for all BD spectra except for one, ranging from 75% to 98%, with an average of 87%, an average improvement of more than 20% observability. The one exception to this improvement was the Mexican Margin 1.6–2.0 g/cm^3 in which the observability actually decreased from 85% in the CP to 81% in the BD spectra, however this difference is within the range of estimated uncertainties for both spin counting techniques. Fig. 3 illustrates that despite the differences in C_{obs}, the CP and BD spectra look remarkably similar. The major resonances are the same in each type of spectra, as are the relative proportions of signal in each region. The Mexican Margin bulk sample (bottom of Fig. 3) shows the second-largest differences in spectral characteristics between CP and BD spectra of any of our samples (after Mexican Margin 2.0–2.5 g/cm^3). For this sample, the BD spectrum has 7.0% less total signal in the alkyl region than does the CP spectrum, and the unsaturated and *O*-aryl regions have 3.2% and 2.0% greater signal, respectively. For the Washington Coast samples, these differences never exceed 3.6% of the total signal intensity and average less than 1.5%. The similarities between the BD and CP spectra indicate that for our samples, the CP spectra with their enhanced S/N ratio and resolution are generally representative of the total OC in the sample and can be used to characterize the OC present in our samples.

RESTORE is a technique designed to investigate which types of OC are underrepresented in CP spectra and to determine what the CP spectra would look like if these underrepresented resonances were included in the spectra (Smernik and Oades, 2003). These summed "total" RESTORE spectra observe almost all the OC, similar to BD spectra, but have the improved resolution and S/N ratio of a CP spectrum. Unfortunately, this technique is extreme-

Table 2
Cross polarization (CP) and Bloch decay (BD) percent carbon observabilities (C_{obs}), average $T_{1\rho}H$ and T_1H values, fast and slow T_1H values and relative abundance of rapidly and slowly relaxing components based on proton spin relaxation editing (PSRE) analysis

Sample	C_{obs} − CP (%)	C_{obs} − BD (%)	$T_{1\rho}H$[a] (ms)	T_1H_{avg}[a] (ms)	T_1H_{fast}[a] (ms)	T_1H_{slow}[a] (ms)	Fast:slow[a]
Washington Slope							
Bulk	57	98	2.82	14.6	11.1	134.2	78:22
Density fractions							
>2.5 g/cm^3	—	—	—	—	—	—	—
2.0–2.5 g/cm^3	62	79	2.85	12.8	N/A	N/A	N/A
1.6–2.0 g/cm^3	68	95	—	—	—	—	—
<1.6 g/cm^3	64	84	3.78	66.2	25.7	159.1	40:60
Size fractions							
<1 μm	71	80	3.09	32.1	N/A	N/A	N/A
<3 μm	60	75	—	—	—	—	—
3–17 μm	65	86	3.15	19.7	8.8	31.2	36:64
17–63 μm	35	—	—	—	—	—	—
>63 μm	—	—	—	—	—	—	—
Mexican Margin							
Bulk	52	94	3.12	8.1	5.6	22.6	72:28
Density fractions							
>2.5 g/cm^3	—	—	—	—	—	—	—
2.0–2.5 g/cm^3	73	95	—	—	—	—	—
1.6–2.0 g/cm^3	85	81	—	—	—	—	—
<1.6 g/cm^3	79	90	—	—	—	—	—
Size fractions							
<1 μm	77	88	3.39	52.1	N/A	N/A	N/A
<3 μm	59	90	—	—	—	—	—
3–17 μm	65	87	2.97	21.5	8.9	29.0	26:74
17–63 μm	56	—	—	—	—	—	—
>63 μm	70	—	—	—	—	—	—

N/A indicates that a two-component PSRE fit was no better than a one-component fit for these samples. Dashes indicate that analyses were not performed on those samples.

[a] $T_{1\rho}H$, proton spin lattice relaxation in the rotating reference frame time constant; T_1H, proton spin lattice relaxation time constant; fast:slow, ratio of rapidly to slowly relaxing PSRE components.

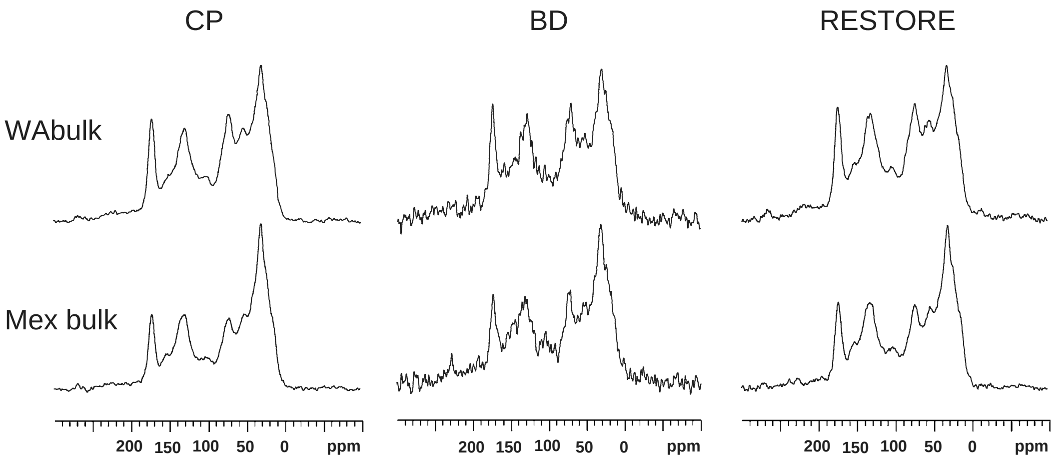

Fig. 3. Comparisons of cross polarization (CP), Bloch decay (BD) and summed RESTORE NMR spectra for the Washington Coast bulk (top) and the Mexican Margin bulk (bottom) sediments.

ly time-consuming and can generally be applied to only a subset of samples. ^{13}C nuclei are commonly underrepresented in CP spectra for two primary reasons: (i) slow rates of magnetization transfer from ^1H to ^{13}C nuclei (long cross polarization time, T_{CH}) that lead to incomplete transfer of polarization to ^{13}C nuclei, and (ii) rapid $T_{1\rho}H$ (proton spin lattice relaxation in the rotating frame) relaxation rates which lead to signal relaxation before measurement of the signal. RESTORE generates three subspectra representative of types of carbon with different combinations of $T_{1\rho}H$ and T_{CH}: (i) C_{SS}, which has short T_{CH} and $T_{1\rho}H$, (ii) C_{SL}, which has a short T_{CH} and a long $T_{1\rho}H$, ideal conditions that lead this fraction to be well-represented in CP spectra, and (iii) C_{LL}, which has long T_{CH} and $T_{1\rho}H$. Both C_{SS} and C_{LL} fractions are underrepresented in CP spectra.

We analyzed three of our samples using the RESTORE technique to probe what types of carbon are underrepresented in our CP spectra and why this is so. Both of our bulk samples contain 34% of their carbon in the C_{SS} fraction, ~50% in the C_{SL} fraction and another ~16% in the C_{LL} fraction, whereas the Washington <1.6 g/cm^3 fraction has 22% C_{SS}, 58% C_{SL} and 21% C_{LL} (Table 3). Note that the Washington <1.6 g/cm^3 fraction has both a higher proportion of C_{SL} carbon and a higher CP observability than the other samples, as might be expected. Fig. 4 shows the spectra for all three subfractions of our samples. The major components of the three subspectra for the two bulk samples are remarkably similar, although the relative proportions of the different resonances vary somewhat between the samples. As has been found in many soils, the C_{SS} components of both samples are dominated by *O*-alkyl and carbonyl resonances, indicating that the short $T_{1\rho}H$ times probably result from binding of paramagnetic cations to these oxygenated functional groups (Smernik and Oades, 2003). The C_{SL} subspectra resemble the CP spectra, whereas unsaturated/aromatic and alkyl signals dominate

Table 3
T_{CH} and $T_{1\rho}H$ values and distribution of carbon between the three RESTORE subfractions

Sample	T_{CH} (short)[a]	T_{CH} (long)[a]	$T_{1\rho}H$ (short)[a]	$T_{1\rho}H$ (long)[a]	% C_{SS}[a]	% C_{SL}[a]	% C_{LL}[a]
Washington Slope							
Bulk	0.20	3.43	0.83	3.06	34	51	15
<1.6 g/cm^3	0.20	4.49	0.76	3.85	22	58	21
Mexican Margin							
Bulk	0.20	2.80	0.81	2.92	34	49	17

[a] T_{CH}, cross polarization time constant; $T_{1\rho}H$, proton spin lattice relaxation in the rotating frame time constant; %C_{SS}, percent of carbon with short T_{CH} and $T_{1\rho}H$; %C_{SL}, percent of carbon with short T_{CH} and long $T_{1\rho}H$; %C_{LL}, percent of carbon with long T_{CH} and $T_{1\rho}H$.

Table 4
Distribution of CP intensity between different spectral regions

Sample	Spectral region (ppm range)							
	% Alkyl C (0–45)	% *N*-Alkyl and methoxyl C (45–60)	% *O*-Alkyl C (60–95)	% Di-*O*-Alkyl C (95–110)	% Unsaturated C (110–145)	% *O*-Aryl C (145–165)	% Carbonyl and amide C (165–190)	% Ketone C (190–215)
Washington Slope								
Bulk	28.3	9.6	18.4	4.8	20.8	6.6	10.2	1.3
Density fractions								
>2.5 g/cm^3	—	—	—	—	—	—	—	—
2.0–2.5 g/cm^3	34.3	10.9	17.5	4.0	17.2	5.0	10.1	0.9
1.6–2.0 g/cm^3	32.2	10.4	17.8	4.2	18.5	5.5	10.2	1.1
<1.6 g/cm^3	24.7	8.1	13.2	5.1	30.9	9.3	7.3	1.5
Size fractions								
<1 μm	32.7	10.1	19.4	4.3	17.1	4.9	10.5	1.1
<3 μm	28.6	9.9	18.2	4.7	21.3	6.2	10.0	1.1
3–17 μm	27.6	9.5	17.8	4.8	22.4	6.8	9.9	1.2
17–63 μm	17.7	7.7	16.6	5.3	29.9	10.8	9.3	2.7
>63 μm	—	—	—	—	—	—	—	—
Mexican Margin								
Bulk	34.1	9.5	15.5	4.4	20.1	6.3	8.8	1.3
Density fractions								
>2.5 g/cm^3	—	—	—	—	—	—	—	—
2.0–2.5 g/cm^3	35.3	9.4	16.5	4.2	17.6	6.0	9.9	1.1
1.6–2.0 g/cm^3	33.8	9.8	17.3	4.4	17.9	5.5	9.9	1.3
<1.6 g/cm^3	34.4	8.9	13.8	4.1	21.6	6.8	8.7	1.6
Size fractions								
<1 μm	38.3	9.9	14.9	3.6	17.2	5.1	9.6	1.4
<3 μm	34.3	10.1	17.9	4.3	17.8	5.1	9.4	1.2
3–17 μm	34.5	9.8	16.9	4.4	18.3	5.5	9.6	1.1
17–63 μm	29.0	9.8	16.4	4.2	19.7	7.1	12.4	1.4
>63 μm	34.8	11.6	13.8	4.0	16.9	6.0	12.2	0.7

Dashes indicate that analyses were not performed on those samples.

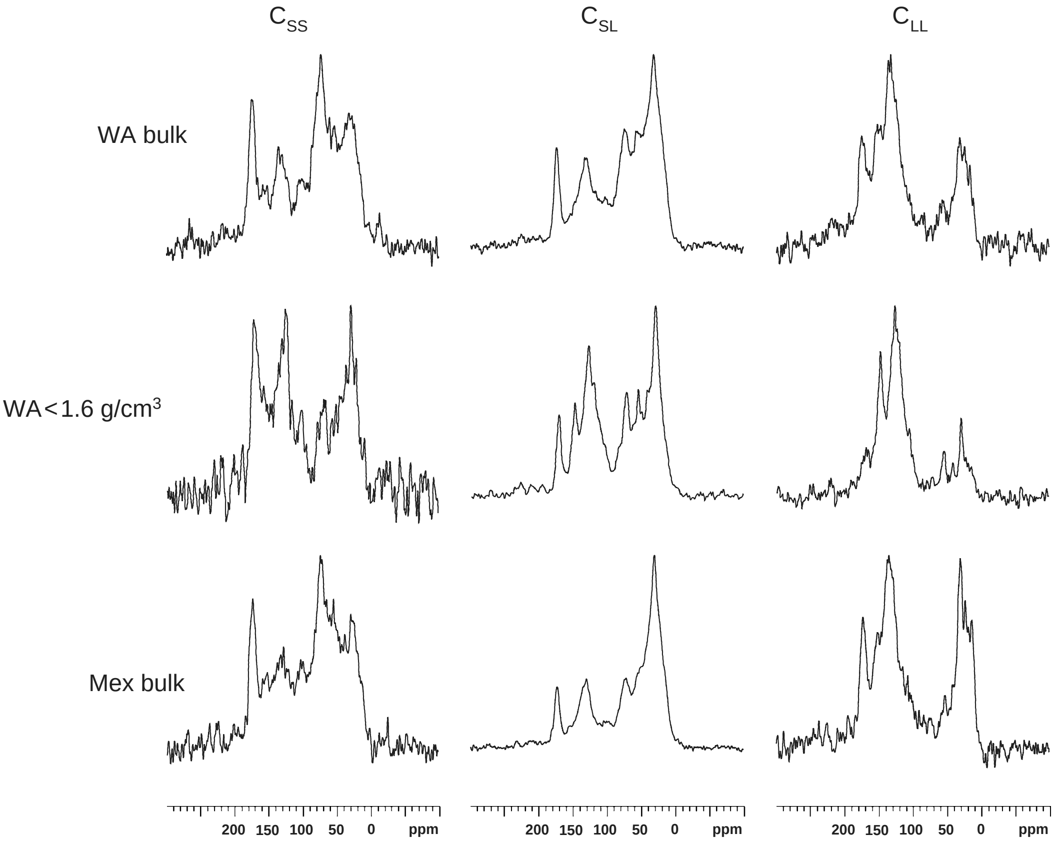

Fig. 4. RESTORE subspectra for the Washington Coast bulk (top), Washington light fraction (middle) and Mexican Margin bulk (bottom) sediments. Subfractions correspond to carbon with short T_{CH} and $T_{1\rho}H$ (C_{SS}, left), short T_{CH} and long $T_{1\rho}H$ (C_{SL}, middle), and long T_{CH} and $T_{1\rho}H$ (C_{LL}, right).

the C_{LL} subspectra for the two samples. The alkyl signal in the C_{LL} subspectra of soils has been ascribed to mobile alkyl structures and the unsaturated signal to black carbon (Smernik and Oades, 2003). However, the Mexican Margin sample contains little terrestrial OC (Ganeshram et al., 1999) and therefore is likely to contain very little black carbon, so some other forms of unsaturated OC with a long T_{CH} may be present in this sample. All three subspectra for the Washington light fraction contain strong unsaturated resonances. The dominantly unsaturated signal in the C_{LL} fraction probably results from the presence of black carbon in this fraction, and the unsaturated signal in the C_{SS} fraction may indicate the presence of some protonated black carbon, which may also have short $T_{1\rho}H$ relaxation rates (Smernik et al., 2002a,b). As shown, the two different mechanisms causing bias in CP spectra affect different types of OC (C_{SS} and C_{LL}). Somewhat fortuitously, the weighted sums of these two underrepresented carbon types is reasonably similar to the well-represented C_{SL} spectra, implying that there should be little overall bias in the CP spectra. Summing all three subspectra together yields the total RESTORE spectra shown in Fig. 3. A comparison of these summed spectra with the CP spectra provides further evidence that while the most representative spectra record somewhat different proportions of resonances (i.e., slightly less alkyl carbon compared with unsaturated), the overall shape and structure of the CP spectra are reasonably indicative of the total spectra and can be used to study the structure of the total OC.

3.4. CP Spectra

3.4.1. Washington Coast fractions

Fig. 5 shows the CP spectra we collected for the Washington Coast samples and Table 4 lists the distribution of spectral areas from the integrated spectra. There was not enough OC in either the densest (>2.5 g/cm^3) or the largest (>63 μm) fractions to allow collection of CP spectra for these fractions. The spectrum of the bulk sediment is dominated by the alkyl carbon signal, which accounts for 28.3% of the total spectral intensity, followed by unsaturated (20.8%), *O*-alkyl (18.4%) and carbonyl/amide (10.2%) resonances (Table 4). Spectra for the densest two fractions look similar to the spectrum for the bulk sample but contain relatively more alkyl carbon and less of other resonances, particularly unsaturated carbon (Fig. 5). In contrast, the light (<1.6 g/cm^3) fraction shows strong unsaturated (30.9%) and *O*-aryl (9.3%) signals but contains only 24.7% alkyl carbon (Table 4). The smallest size fractions look very similar to the densest fractions, with a strongly dominant alkyl peak, and the largest fraction resembles the light fraction with a strong unsaturated resonance but somewhat more *O*-alkyl carbon than found in the <1.6 g/cm^3 fraction (Fig. 5). Unfortunately, the 17–63 μm fraction contained

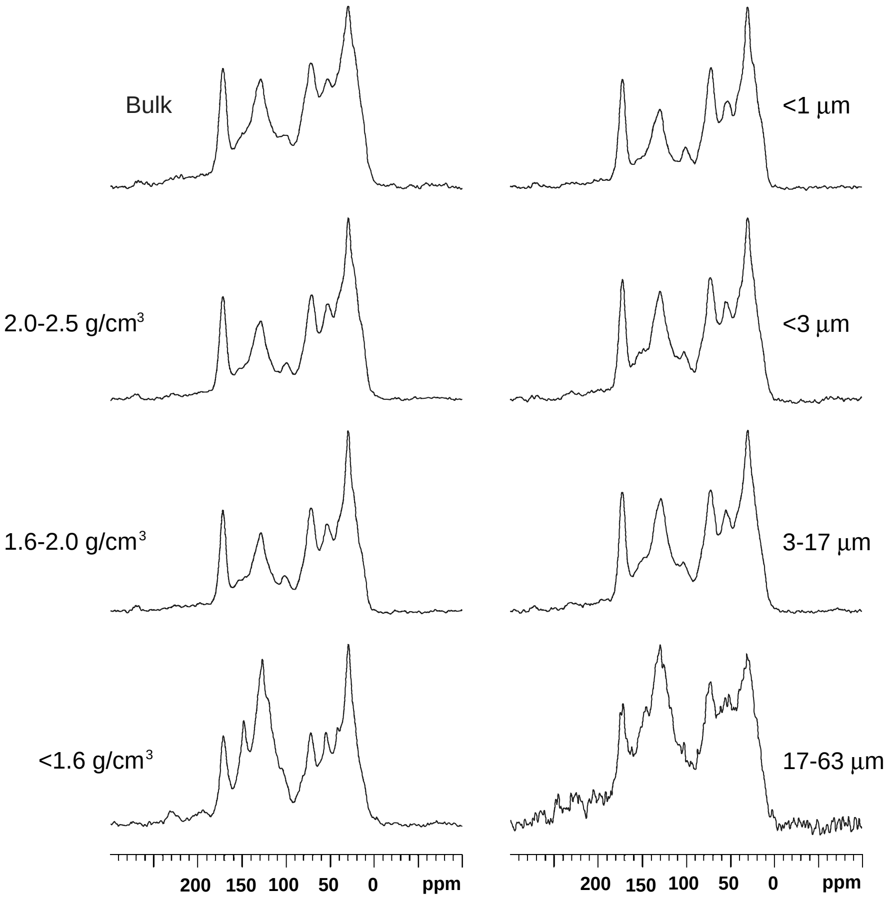

Fig. 5. CP spectra for the Washington Coast sediment fractions. The bulk sediment and density fractions are on the left and the size fractions are on the right.

very little OC (~12 mg), and thus its CP spectrum has a relatively low S/N ratio and is not as clean as those for the other samples.

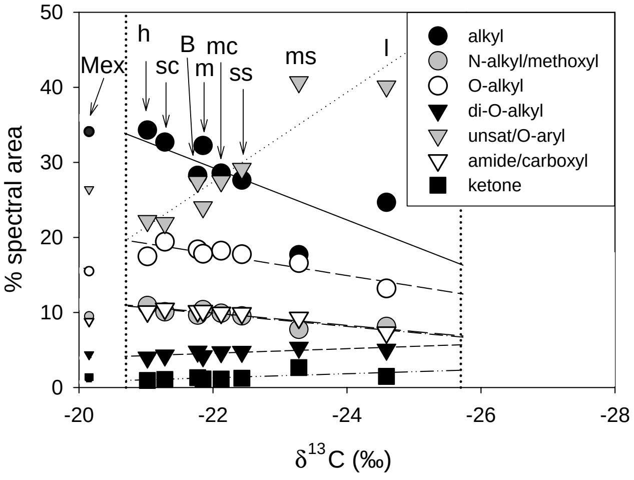

Fig. 6. Plot of integrated areas of the NMR spectra for the Washington Coast sediment fractions plotted versus stable carbon isotopic signature of the fractions. Sample labels are as given in Table 1. The areas for the Mexican Margin bulk sample are plotted as small symbols for reference. R^2 values for the regression lines are: alkyl = 0.58, *N*-alkyl/methoxyl = 0.78, *O*-alkyl = 0.78, di-*O*-alkyl = 0.63, unsat/*O*-aryl = 0.87, amide/carboxyl = 0.88, ketone = 0.33. The dotted vertical lines mark isotopic values representative of marine (−20.7‰) and terrestrial (−25.7‰) OC, as discussed in Section 3.2.

The spectra show similar trends of decreasing alkyl signal and increasing unsaturated and *O*-aryl signals moving from dense to light fractions and from small to large fractions (Fig. 5; Table 4). Fig. 6 shows that these resonances mix approximately linearly when the spectral areas of the resonances are plotted versus the stable carbon isotopic signature. For this plot we combined unsaturated and *O*-aryl carbon because the two regions were highly correlated. The slopes of all lines are statistically significant and four of the seven lines are highly correlated ($R^2 = 0.78$–0.88; Fig. 6). The strongest trend in Fig. 6 is increasing contribution of unsaturated/*O*-aryl carbon as the OC becomes more ^{13}C-depleted. This relative gain of unsaturated OC ($m = -6.0$ area%/‰; $R^2 = 0.87$) derives primarily from decreases in the contribution of alkyl OC ($m = 3.5$ area%/‰; $R^2 = 0.58$), as well as from smaller decreases in *O*-alkyl, *N*-alkyl/methoxyl and amide/carboxyl OC resonances (Fig. 6). Di-*O*-alkyl and ketone OC increase slightly with increasing ^{13}C depletion, but these are both relatively minor components of the total spectra and do not vary as dramatically as do the other components. All correlations are improved by or do not change with the exclusion of the 17–63 μm sample, which falls off of most of the lines with considerably more unsaturated and less alkyl OC than predicted by the lines for the measured δ^{13}C signature. We observed only 35% of the OC in this sample using CP, just over half of the carbon typically observed for these samples, and were not able to collect a BD spectrum, so it is likely that the CP spectrum for this sample is not representative of the total OC in this sample, which may account for its divergence from the lines in Fig. 6.

The linearity of most of the plots of spectral areas against $\delta^{13}C$ signature (Fig. 6) confirms that the OC in these sediment fractions results from linear mixing between two different carbon endmembers. The marine endmember would lie to the left of the plot near the dotted line marking the $\delta^{13}C$ signature for marine OC (−20.7‰) calculated in Section 3.2 (Fig. 6). This marine OC is dominant in the small and dense fractions and contains large amounts of alkyl carbon and relatively little unsaturated and *O*-aryl carbon. The terrestrial endmember would lie to the right, near the dotted line marking the terrestrial OC $\delta^{13}C$ signature (−25.7‰; Fig. 6), predominates in the large and light fractions and contains roughly half of its carbon in unsaturated structures with relatively little alkyl OC.

3.4.2. Mexican Margin fractions

Fig. 7 shows the CP spectra collected for the Mexican Margin samples and Table 4 lists the distribution of spectral areas from the integrated spectra. The >2.5 g/cm^3 fraction did not contain enough carbon for a CP spectrum. We did collect spectra for the 17–63 and >63 μm fractions, however, both of these samples lost half or more of their OC (~50% and ~80%, respectively) during demineralization, so the spectra collected for these fractions may not be representative of the total OC in these fractions. The bulk sediment contains relatively more alkyl carbon than does the Washington Coast bulk sediment and relatively less of all other types of carbon (Fig. 7). All of the density and size fractions look very similar to the bulk sediment, with no dramatic differences or trends between the samples; alkyl carbon dominates all of the spectra. Whereas the density fractions show essentially no trends, the size fractions show slight trends towards increasing unsaturated and decreasing alkyl carbon with increasing size (Table 4). Con-

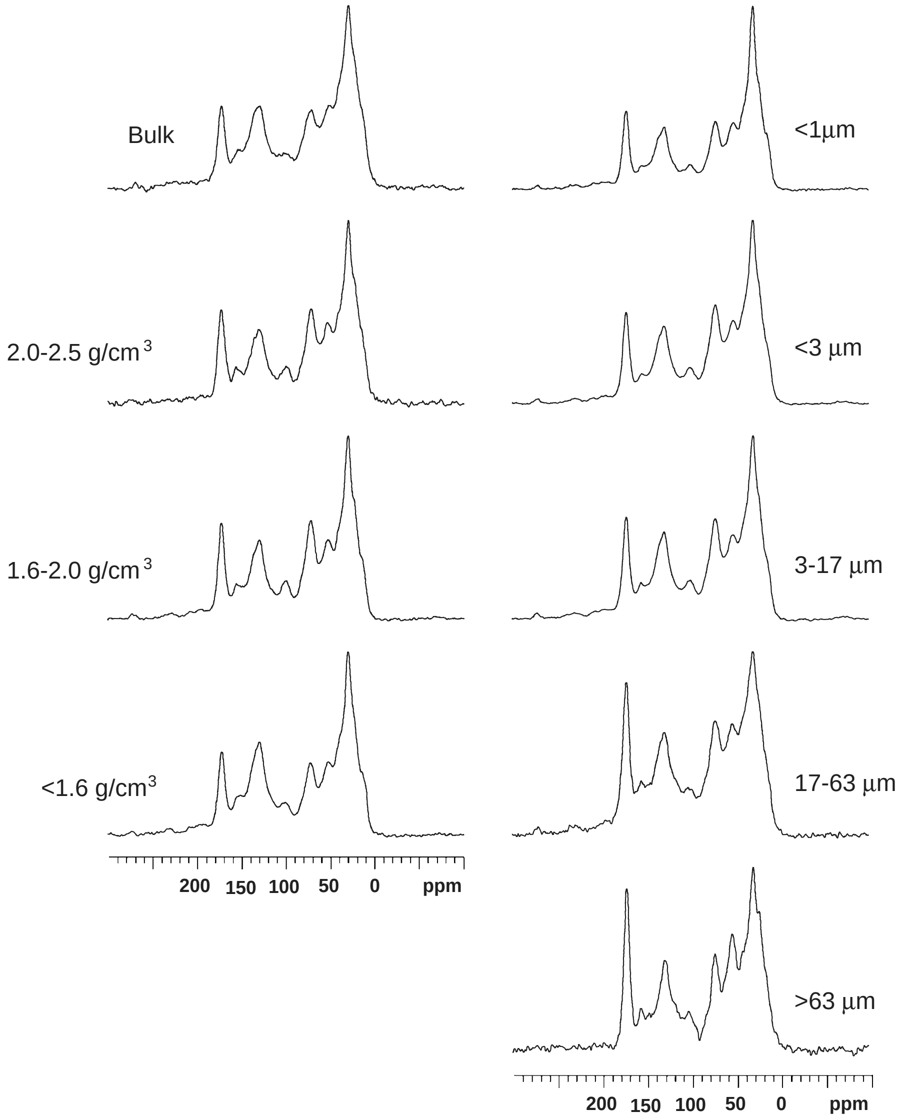

Fig. 7. CP spectra for the Mexican Margin sediment fractions. The bulk sediment and density fractions are on the left and the size fractions are on the right.

sidering only the three smallest size fractions (because the largest two are not likely to be representative), these changes amount to a 1.1% change in the unsaturated region and a 3.8% change in the alkyl region. Compared with the 5.1% and 5.3% changes in these size fractions for the Washington Coast sediments, these trends are relatively minor, and in general, the OC in the Mexican Margin sediment fractions appears very alkyl-rich and homogenous. Plotting the spectral areas for the Mexican Margin bulk sample with the Washington Coast data shows that the Mexican Margin sample plots to the far left of the graph, with spectral areas that are near to most of the lines but are considerably enriched in unsaturated carbon and depleted of *O*-alkyl OC relative to the predicted values based on the Washington Coast sediment fractions (Fig. 6).

3.5. Proton spin relaxation editing

We analyzed half of the Washington Coast sediment fractions and three Mexican Margin fractions using proton spin relaxation editing (PSRE) to investigate the spatial and chemical heterogeneity of carbon within our sediments. Proton spin relaxation rates of different nuclei are homogenized within a sample by spin diffusion, a process in which the relaxation of one proton leads to relaxation of nearby protons. This process is efficient on spatial scales of less than 100 nm (Zumbulyadis, 1983), so that within-sample heterogeneity on a scale greater than this may lead to non-uniform T_1H values within a sample. PSRE is a technique that separates slowly and rapidly relaxing components of a sample based on the inversion-recovery experiment (Newman and Tate, 1991; Preston and Newman, 1992). These two PSRE subspectra are indicative of structures that are, on average, physically distinct and spatially isolated within a sample. The magnitude of the T_1H values for both the average carbon and the two subfractions are affected by the amount of paramagnetic cations remaining in the sample after demineralization and are very sensitive to moisture content (Newman, 1992; Hatcher and Wilson, 1991), so the absolute values of T_1H may not be that meaningful.

Within the Washington Coast sediments, the most marine samples (<1 μm and 2.0–2.5 g/cm^3) model best as one component (Table 2), suggesting that the OC in these fractions is homogenous at the 100-nm scale. This marine-derived component may therefore contain either just one type of OC or, more likely, many types of OC (e.g., proteins and lipids) that are physically mixed on a <100 nm scale. In contrast, PSRE separates the OC in the most terrestrial sample (<1.6 g/cm^3) into two components at a 40:60 ratio of rapidly to slowly relaxing carbon (Table 2). The subspectra for these components show that the terrestrial OC in this environment is not homogeneous at the 100 nm size scale and contains a mixture of different types of OC (Fig. 8). The rapidly relaxing component is dominated by a strong unsaturated carbon signal, probably derived from aromatic-rich charcoal, which tends to have very short T_1H values (Golchin et al., 1997a; Smernik et al., 2000; Golding et al., 2004), along with alkyl carbon. The sharp *O*-aryl and *N*-alkyl/methoxyl resonances present in the slowly relaxing component, along with a strong unsaturated signal (Fig. 8), are diagnostic of lignin (see later discussion and Fig. 9). The alkyl OC and other resonances in this subspectrum may derive from the presence of marine carbon in this fraction (this sample modeled as 22% marine OC). The Washington Coast 3–17 μm fraction contains a more even mixture of the marine and terrestrial endmembers. The slowly relaxing PSRE component of this sample closely resembles the spectra of the marine-dominated samples, with a dominant alkyl peak (Fig. 8). The rapidly relaxing component is rich in unsaturated carbon and may represent an average of the two subspectra from the dominantly terrestrial <1.6 g/cm^3 fraction, although it contains more carbonyl and *O*-alkyl resonances (Fig. 8). Interestingly, this rapidly relaxing component accounts for a similar percentage of the total OC as was modeled to be terrestrial using isotopes (35%; Table 1). For the bulk Washington Coast sample, the two PSRE components have similar distributions of resonances, and this technique does not effectively separate terrestrial from marine OC in this sample (Fig. 8).

PSRE separates the bulk Mexican Margin sample into two components in a 72:28 ratio of rapidly to slowly relaxing carbon (Table 2). The rapidly relaxing component looks like the other marine fractions, whereas the slowly relaxing component is dominated by a large alkyl peak, probably due to the presence of large amounts of polymethylenic carbon, which is typically very slowly relaxing (Fig. 8; Smernik et al., 2000). Accumulation of such alkyl-rich material in the Mexican Margin sample, which has been exposed to little oxidative degradation, has been shown before (Gélinas et al., 2001a) and is consistent with the accumulation of algaenans or other lipids (Gelin et al., 1996). The Mexican <1 μm fraction models as one component, but the 3–17 μm fraction models better as two components than as one (Table 2). However, the subspectra for this latter fraction contained some "valleys" in the spectra, notably at 30 ppm, the normal peak for alkyl carbon (Fig. 8), that suggest that the two subspectra are distorted and that this fraction would model better as three components.

3.6. Mixing of endmembers in sediments

Stable carbon isotopes, N/C ratios, lignin analysis and NMR spectra all suggest that the Washington Coast sediments contain a mixture of two dominant endmembers. In contrast, the Mexican margin sediments appear to contain primarily one relatively homogeneous type of organic matter. It is likely that none of the sediment fractions from the Washington slope sediment are composed purely of one endmember or the other, however, we can infer the chemical properties of each endmember by examining the NMR spectra of samples that lie to each end of the mixing plots (Figs. 2 and 6). These pseudo-endmember spectra are shown at the top of Fig. 9. The terrestrial endmember here is represented by the light fraction from the Washington

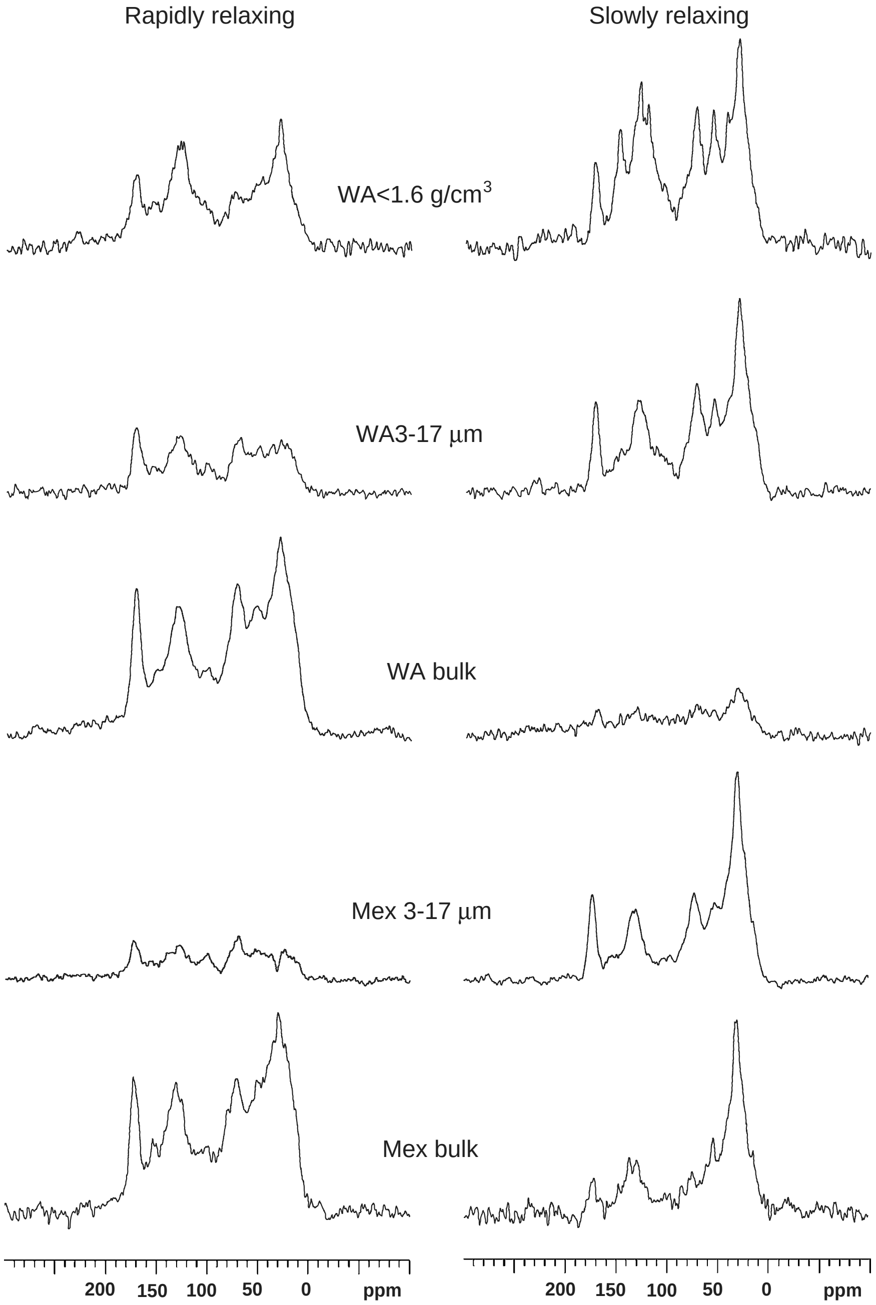

Fig. 8. Proton spin relaxation editing subspectra for all samples for which a two-component mixture was tried and proved meaningful. The rapidly relaxing component is shown on the left and the slowly relaxing component is on the right. Subspectra are normalized so that the area under each curve is proportional to the amount of OC present in that component.

coast sediment, which looked the most terrestrial based on isotopic, elemental, lignin and NMR spectroscopic analyses and modeled as 78% terrestrial based on ^{13}C isotopes (Table 1). This terrestrial "near-endmember" is dominated by a large unsaturated peak and has a relatively small alkyl peak (Fig. 9). It also has very sharp *O*-aryl and *N*-alkyl/methoxyl peaks that are diagnostic of lignin, as shown in the lignin spectrum below it (Fig. 9). The large ratio of unsaturated to *O*-aryl carbon suggests the additional presence of combustion-derived black carbon (BC), which is dominated by aromatic carbon as shown in the charcoal spectrum (Fig. 9). The dominance of BC and lignin in the terrestrial endmember agrees with the lignin data showing that lignin biomarkers are considerably enriched in the largely terrestrial light and large fractions and is also consistent with the inherently low density of BC (Goldberg, 1985). The PSRE analysis further supports large BC and lignin contributions to the terrestrial endmember.

We used a molecular mixing model (Nelson et al., 1999; Hedges et al., 2002; Baldock et al., 2004) based on the CP spectrum of this sample and of known biochemicals to estimate the concentrations of lignin and BC (modeled as charcoal) in our terrestrial pseudo-endmember. The model estimates that the <1.6 g/cm^3 fraction contains 36% char-

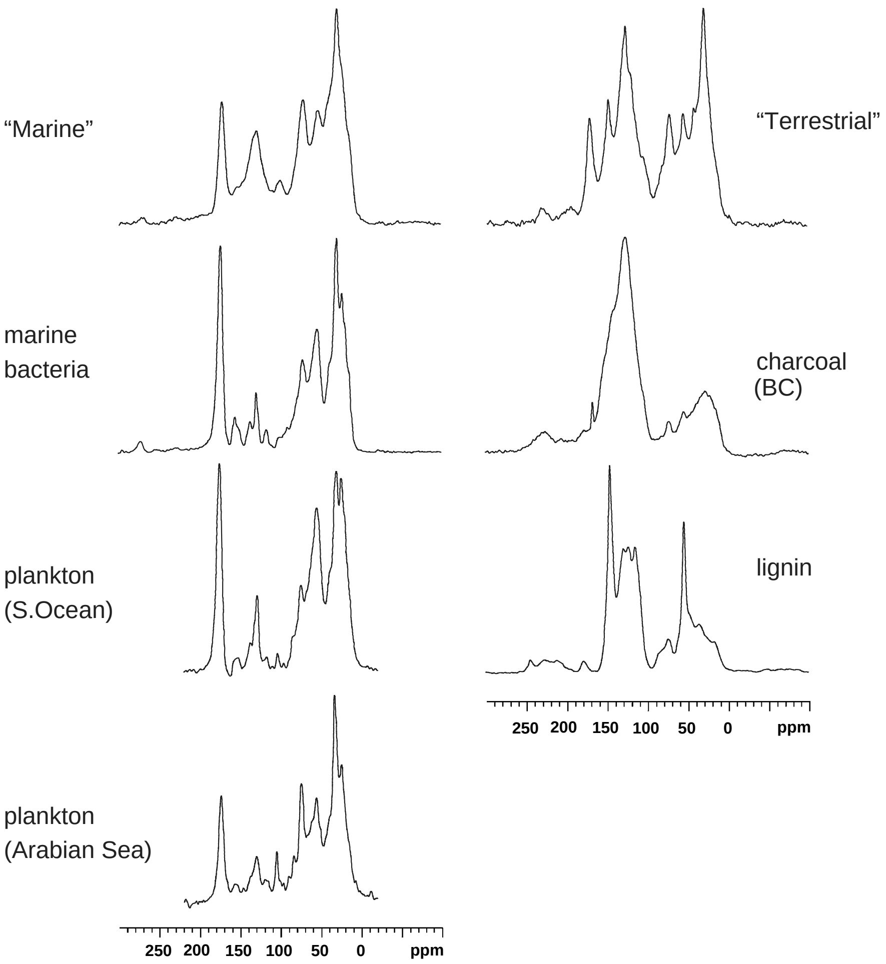

Fig. 9. Spectra of possible carbon endmembers and sources. The top two spectra show samples that lie nearest an endmember (left: WA 2.0-2.5 g/cm^3—marine endmember; right: WA <1.6 g/cm^3—terrestrial endmember). The lower plots show possible sources of this carbon for comparison of the NMR spectra. The two plankton spectra are redrawn from Hedges et al. (2002).

coal-BC and 17% lignin carbon. The remaining carbon is divided between proteins, carbohydrates and lipids. The light fraction accounts for approximately 17% of the total OC in the sediment, and if roughly one third of this carbon is BC, that BC would comprise at least 6% of the total OC (ignoring any BC in denser fractions), which is within the range of BC concentrations observed using other methods for continental margin sediments (Kuhlbusch, 1998; Masiello, 2004). The modeled lignin concentration is considerably higher than the 3.6% of TOC measured by cupric oxide oxidation (Table 1), but this higher concentration is supported by the large size and sharpness of the *O*-aryl and *N*-alkyl/methoxyl peaks (Fig. 9). Additionally, cupric oxide oxidation is a known to significantly underestimate lignin concentrations (Goñi and Hedges, 1992; De Montigny et al., 1993; Hatcher et al., 1995). PSRE analysis suggests that this light fraction contains a "marine-like," alkyl-rich component as well, which accounts for the presence of the alkyl and carboxyl carbon evident from the spectra. The presence of this carbon along with the lignin and charcoal is consistent with the δ^{13}C and N/C signatures indicating a mixture of terrestrial and marine carbon in this fraction. However, approximately half of the NMR intensity in the light fraction cannot be accounted for by charcoal or lignin according to the model, whereas only about 22% of the OC appears to be marine based on its isotopic signature (Table 1). This suggests that some of the alkyl carbon may come from alkyl-rich terrestrial sources such as debris from soil bacteria, cutin or suberin, but the large uncertainties inherent in both of these estimates prevent an accurate assessment of the importance of this possible third source of terrestrial OC.

We used the Washington Coast 2.0–2.5 g/cm^3 fraction to represent the marine endmember in Fig. 9. This component has a strong alkyl signal, along with smaller resonances in the *O*-alkyl, unsaturated and carbonyl regions. All Mexican Margin sediments are dominated by this type of carbon, and all have spectra that look very similar (Fig. 7). This carbon also appears to be similar to the "marine-like" carbon present in the small and dense fractions of the WA margin sediment (Fig. 5). Additionally, Gélinas et al. (2001a) found similar spectra in at least four additional locations around the world, although the OC in highly oxidized sediments (i.e., open-ocean environments) had very different spectra. In short, this alkyl-rich material appears to be a sort of ubiquitous "marine" OC present in all size and density fractions of sediments and in most continental margin environments. In Fig. 9, we compare this material with NMR spectra of several likely sources of this marine OC: plankton and gram-negative marine sedimentary bacteria. The plankton samples have strong amide/carboxyl, *N*-alkyl and alkyl (including a methyl peak around 20 ppm) resonances characteristic of protein carbon, as well as *O*-alkyl carbon from carbohydrates. The spectra of the two plankton samples have been interpreted to contain varying amounts of protein and carbohydrate carbon, with proteins dominating in the Southern Ocean sample and carbohydrates and lipids relatively more important in the Arabian Sea sample (Hedges et al., 2002). The bacterial sample has an NMR spectrum intermediate between these two, with large signals from amide/carboxyl, *N*-alkyl and alkyl carbon, as well as a significant *O*-alkyl peak and a methyl peak (within the alkyl range at around 23 ppm), reflecting its main biochemical constituents, namely proteins, carbohydrates and lipids. In comparison with these pure sources of marine OC, the marine pseudo-endmember contains much more unsaturated carbon and does not show a distinct methyl peak. It also appears to contain fewer proteins (less amide and *N*-alkyl carbon) than the bacteria and Southern Ocean plankton samples. It is possible that the unsaturated signal in the sediments derives from the presence of small amounts of BC or lignin (as evident from lignin biomarkers). However, the presence of unsaturated carbon in the Mexican Margin sample, which contains little terrestrial OC, makes this unlikely as the dominant source of unsaturated OC. Another possibility is that this unsaturated carbon could derive from small amounts of kerogen present within the mineral matrix of the sediments. Such kerogen generally has NMR spectra dominated by unsaturated and alkyl resonances (Petsch et al., 2001; Werner-Zwanziger et al., 2005) and has been found in modern sedimentary environments (e.g., Blair et al., 2003). Based on this comparison, the "marine" carbon does not consist of unaltered plankton or bacterial biomass; instead these marine sources of carbon must be (bio)chemically processed before burial in marine sediments and could partly derive from old, recycled petrogenic sources.

3.7. Implications for black carbon distribution

This study finds that most of the BC is in the large and light fractions of the Washington Coast sediment. The low density of the BC implies that, unlike in soils (Golchin et al., 1997b; Glaser et al., 2000) it is not associated with sedimentary minerals in this environment. The large size of the BC indicates that larger charcoal particles dominate over smaller, submicron soot particles (Goldberg, 1985). The low density of the particles will facilitate their distribution throughout the ocean.

In another study, we found that graphitic black carbon (GBC, operationally defined as the carbon resistant to thermal oxidation following chemical pretreatment) is concentrated in the dense and silt-sized fractions of the same Washington Coast sediment and concluded that this type of highly condensed BC was rock-derived (Dickens et al., 2004). This fossil GBC is presumably highly aromatic, but it comprises a small enough proportion of the total OC in each fraction (<1.5% of TOC in the small and dense fractions and always <5.2% of TOC) that it would not contribute significantly to the unsaturated/aromatic resonances of the samples. Comparing the very different distributions of these two types of BC in the same sediment fractions is further proof of the extreme heterogeneity of the materials labeled "black carbon" and indicates that these different forms of BC are likely to follow very different distribution pathways throughout the environment.

3.8. Preservation mechanisms of OC in sediments

Sediments from the Washington Margin are subject to substantial and prolonged oxic degradation, both during transport to their ultimate burial site and while residing in surface marine sediment horizons (Hedges et al., 1999; Keil et al., 2004). Because of this, OC in these sediments may be highly altered. In contrast, the sediments within the Mexican Margin oxygen-deficient zone (ODZ) undergo less intense degradation due to the absence of oxygen in the overlying waters (Hartnett et al., 1998). Hartnett and Devol (2003) estimate that in the Mexican Margin ODZ, >15% of marine primary production reaches the sediments and ~8% survives degradation in surface sediments to be buried in deep sediments, as compared with <8% and ~1.2%, respectively, for the Washington Margin. This difference in degradation extent between the two environments means that mechanisms protecting different forms of OC might be relatively more important and more apparent within the Washington Coast sample than in the Mexican Margin sample. We can investigate the contribution of different preservation mechanisms in these sediments by comparing the OC character and associations in these two different locations.

We find that most of the OC in the Washington Coast sediment that is recognizably terrestrial appears to be lignin and charcoal that is largely unassociated with minerals (Fig. 9). There is little evidence in this sediment for the presence of large amounts of soil OC, although it is apparent in other environments (e.g., Gordon and Goñi, 2003) and even in other sediments from this region (Keil et al., 1994b; Prahl et al., 1994). Our finding that very little mineral-associated terrestrial OC was preserved in the Washington Coast sediment suggests that mineral-association does not efficiently preserve the terrestrial OC. Instead, selective preservation of (bio)chemically recalcitrant lignin and charcoal appears to be the primary mechanism preserving terrestrial OC in this sediment.

The mechanisms protecting marine OC from degradation in these sediments remain somewhat more obscure, but our characterization of the OC quality and mineral associations provides insight into them. Within the Washington Coast, we found that the vast majority of the marine

OC was in relatively small fractions and closely associated with sedimentary minerals (>2.0 g/cm^3), with only a small amount present in the large and light fractions. In contrast, marine OC was in all size and density fractions of the Mexican Margin sample, and most of it was in the relatively light mineral-associated (1.6–2.0 g/cm^3) and <3 μm clay fractions (Fig. 1). In both environments, most of the minerals are lithogenic, so most of the marine OC in these sediments is associated with continentally derived minerals. The two environments contain similar types of terrigenous minerals (smectite, albite, orthoclase and quartz; Keil et al., 1994b; Arnarson and Keil, 2001; Gélinas et al., 2001b) and presumably have similar, dominantly planktonic sources of OC but differ dramatically in terms of how much degradation the OC has been subjected to (Hartnett and Devol, 2003). These conditions mean that comparing the two sites can provide insight into how degradation affects OC quality and association with minerals. From this comparison, we can speculate on the mechanisms preserving this marine OC.

Marine OC in both environments appears to be almost identical by NMR spectroscopy (Figs. 5 and 7), indicating that the overall quality of the OC does not change considerably, even when subjected to the more highly oxidizing conditions of the Washington Margin. This suggests that selective preservation does not play a dominant role in preserving this OC. Indeed, in the Mexican Margin sediment, the homogeneity of the OC in all fractions yields little evidence of either selective preservation or mineral protection. In the mildly degraded Mexican Margin sediment, most (marine) OC is loosely associated with minerals but >20% remains mineral-free (Fig. 1). Additionally, Arnarson and Keil (2001) defined all OC in the <1.9 g/cm^3 fractions as mineral-free and found that ~70% of the OC in a similar Mexican Margin ODZ sediment was unassociated with minerals by this definition. In contrast, in the highly degraded Washington Coast slope sample, virtually all marine OC is associated with minerals, most of it tightly associated. The differences between the mineral association of marine OC in mildly versus highly degraded environments suggests that most of the marine OC that is not associated with minerals is lost during degradation at the Washington Margin site. This in turn indicates that marine OC may survive oxidation in this environment primarily via association with minerals. These conclusions are consistent with those of Hedges et al. (2001) and Minor et al. (2003) who found that nonselective preservation of OC, presumably through mineral association, dominated in sinking marine particles. However, a comparison of the spectra of our marine endmember (Fig. 9) with those of the sinking particles shown in Hedges et al. (2001) shows that the sediments are considerably enriched in alkyl carbon compared with the sinking particles. This sedimentary enrichment in alkyl carbon indicates that selective preservation of marine alkyl carbon may also account for the preservation of some of the OC in the sediments (Hatcher et al., 1983; Hwang and Druffel, 2003), but this preservation appears to occur concurrently with mineral-association. It is unclear why mineral protection appears to be so much more efficient at preserving marine OC than terrestrial OC, but this suggests that these different types of OC may be connected to the minerals via different types and strengths of associations.

4. Conclusions

The combination of elemental and isotopic analyses and NMR spectroscopy applied to physical fractions of sediments is a powerful tool for investigating how different forms of OC are preserved in marine sediments. All of the analyses indicate that the Washington Coast slope sediment contains a mixture of two different types of organic carbon. The first is characteristically marine according to stable carbon isotopes, N/C elemental ratios and its low lignin content. This endmember is concentrated in the small and dense fractions, indicating that it is closely associated with sedimentary minerals, and its NMR spectra are dominated by alkyl carbon. Isotopic, elemental and lignin phenol analyses indicate that the second endmember is terrestrial vascular plant debris. The concentration of this endmember in the light and large fractions shows that it is mostly unassociated with minerals, and unsaturated and *O*-aryl resonances dominate its NMR spectrum. This terrestrial OC seems to consist primarily of lignin and black carbon. In contrast, the Mexican Margin sedimentary OC is homogenous and resembles the Washington slope marine endmember.

It is unclear what mechanisms help preserve OC in the Mexican Margin sediment, but in the Washington Coast slope sediment different mechanisms appear to protect different types of OC. The presence of most of the terrestrial OC in recalcitrant, mineral-free forms suggests selective preservation of these forms of terrestrial OC and corresponding efficient degradation of mineral-associated terrestrial OC. Comparison of the character and mineral associations of marine OC in these two environments, which are subject to dramatically different degrees of degradation, suggests that mineral-protection is the dominant mechanism preserving marine OC in this sediment. The differing abilities of mineral-association to protect marine versus terrestrial OC in this environment suggest that different types of OC-mineral associations may be involved in the two cases. Further work is needed to determine whether the same combination of preservation mechanisms functions in other sediments along this continental margin and within other environments and to further probe the fate of mineral-associated terrestrial OC in the oceans.

Acknowledgments

We acknowledge R. Keil, A. Aufdenkampe and the UW MOG and CSIRO Organic Matter groups for help synthesizing this work and C. Preston, J. Skjemstad, E. Krull, J. Hwang and three anonymous reviewers for helpful comments on this manuscript. D. Wilbur performed the isotopic analyses, and B. Van Mooy helped with the bacterial culture. The Washington Coast sediment was collected with the help of the crew of the R/V *New Horizon* and T. Eglinton's research group. A. Devol and R. Keil collected the Mexican Margin sediment, and C. Masiello provided the charcoal sample. This research was supported by the National Science Foundation (NSF) via a grant to J.I.H. and a Graduate Research Fellowship to A.F.D.

Associate editor: Carol Arnosti

Appendix A

See Table A1.

Table A1
Yields of lignin phenols from the Washington Coast slope sediment

	Concentrations (mg/100 mg OC)							
	Vl[a]	Vn[a]	Vd[a]	Sl[a]	Sn[a]	Sd[a]	Cd[a]	Fd[a]
Bulk	0.39	0.12	0.14	0.14	0.08	0.03	0	0.02
Density fractions								
2.0–2.5 g/cm^3	0.14	0.04	0.07	0.07	0.05	0.02	0.01	0.06
1.6–2.0 g/cm^3	0.27	0.08	0.10	0.16	0.07	0.03	0.02	0.02
<1.6 g/cm^3	1.76	0.46	0.53	0.38	0.11	0.09	0.21	0.06
Size fractions								
<1 μm	0.24	0.08	0.11	0.10	0.09	0.03	0.02	0.09
<3 μm	0.49	0.16	0.18	0.19	0.09	0.05	0	0.03
3–17 μm	0.55	0.16	0.19	0.20	0.08	0.04	0.05	0.03
17–63 μm	0.82	0.20	0.22	0.23	0.06	0.04	0.33	0.03
>63 μm	1.28	0.33	0.31	0.37	0.10	0.07	0.32	0.04

[a] Vl, vanillin; Vn, acetovanillone; Vd, vanillic acid; Sl, syringealdehyde; Sn, acetosyringeone; Sd, syringic acid; Cd, *trans*-coumaric acid; Fd, *trans*-ferulic acid.

References

Alla, M., Lippmaa, E., 1976. High-resolution broad line C-13 NMR and relaxation in solid norbornadiene. *Chem. Phys. Lett.* **37** (2), 260–264.

Arnarson, T.S., Keil, R.G., 2001. Organic-mineral interactions in marine sediments studied using density fractionation and X-ray Photoelectron Spectroscopy. *Org. Geochem.* **32**, 1401–1415.

Arnarson, T.S., Keil, R.G., 2005. Influence of organic-mineral aggregates on microbial degradation of the dinoflaggelate *Scrippsiella trochiodea. Geochim. Cosmochim. Acta* **69** (8), 2111–2117.

Aufdenkampe, A.K., Hedges, J.I., Richey, J.E., Krusche, A.V., Llerena, C.A., 2001. Sorptive fractionation of dissolved organic nitrogen and amino acids onto fine sediments within the Amazon Basin. *Limnol. Oceanogr.* **46** (8), 1921–1935.

Baldock, J.A., Smernik, R.J., 2002. Chemical composition and bioavailability of thermally, altered *Pinus resinosa* (Red Pine) wood. *Org. Geochem.* **33** (9), 1093–1109.

Baldock, J.A., Masiello, C.A., Gélinas, Y., Hedges, J.I., 2004. Cycling and composition of organic matter in terrestrial and marine ecosystems. *Mar. Chem.* **92** (1–4), 39–64.

Berner, R.A., 1989. Biogeochemical cycles of carbon and sulfur and their effect on atmospheric oxygen over Phanerozoic time. *Glob. Planet. Change* **75** (1–2), 97–122.

Blair, N.E., Leithold, E.L., Ford, S.T., Peeler, K.A., Holmes, J.C., Perkey, D.W., 2003. The persistence of memory: the fate of ancient sedimentary organic carbon in a modern sedimentary system. *Geochim. Cosmochim. Acta* **67**, 63–73.

Bock, M.J., Mayer, L.M., 2000. Mesodensity organo-clay associations in a near-shore sediment. *Mar. Geol.* **163** (1–4), 65–75.

Burdon, J., 2001. Are the traditional concepts of the structures of humic substances realistic?. *Soil Sci.* **166** (11) 752–769.

Christensen, B.T., 1992. Physical fractionation of soil and organic matter in primary particle size and density separates. *Adv. Soil Sci.* **20**, 1–90.

De Montigny, L.E., Preston, C.M., Hatcher, P.G., Kögel-Knabner, I., 1993. Comparison of humus horizons from two ecosystem phases of northern Vancouver Island using C-13 CPMAS NMR-spectroscopy and CuO oxidation. *Can. J. Soil Sci.* **73** (1), 9–25.

Derenne, S., Largeau, C., 2001. A review of some important families of refractory macromolecules: composition, origin, and fate in soils and sediments. *Soil Sci.* **166** (11), 833–847.

Derenne, S., Largeau, C., Casadevall, E., Berkaloff, C., Rousseau, B., 1991. Evidence of kerogen formation in source rocks and oil shales via selective preservation of thin resistant outer walls of microalgae: origin of ultralaminae. *Geochim. Cosmochim. Acta* **55**, 1041–1050.

Dickens, A.F., Gélinas, Y., Hedges, J.I., 2004. Physical separation of combustion and rock sources of graphitic black carbon in sediments. *Mar. Chem.* **92** (1–4), 215–223.

Ganeshram, R.S., Calvert, S.E., Pedersen, T.F., Cowie, G.L., 1999. Factors controlling the burial of organic carbon in laminated and bioturbated sediments off NW Mexico: implications for hydrocarbon preservation. *Geochim. Cosmochim. Acta* **63** (11–12), 1723–1734.

Gelin, F., Boogers, I., Noordeloos, A.A.M., Damste, J.S.S., Hatcher, P.G., deLeeuw, J.W., 1996. Novel, resistant microalgal polyethers: an important sink of organic carbon in the marine environment? *Geochim. Cosmochim. Acta* **60** (7), 1275–1280.

Gélinas, Y., Baldock, J.A., Hedges, J.I., 2001a. Organic carbon composition of marine sediments: effect of oxygen exposure on oil generation potential. *Science* **294** (5540), 145–148.

Gélinas, Y., Baldock, J.A., Hedges, J.I., 2001b. Demineralization of marine and freshwater sediments for CP/MAS ^{13}C NMR analysis. *Org. Geochem.* **32**, 677–693.

Giddings, J.C., 1985. A system based on split-flow lateral-transport thin (SPLITT) separation cells for rapid and continuous particle fractionation. *Separ. Sci. Technol.* **20** (9–10), 749–768.

Glaser, B., Balashov, E., Haumaier, L., Guggenberger, G., Zech, W., 2000. Black carbon in density fractions of anthropogenic soils of the Brazilian Amazon region. *Org. Geochem.* **31**, 669–678.

Golchin, A., Baldock, J.A., Clarke, P., Higashi, T., Oades, J.M., 1997a. The effects of vegetation and burning on the chemical composition of soil organic matter of a volcanic ash soil as shown by ^{13}C NMR spectroscopy. II. Density fractions. *Geoderma* **76**, 175–192.

Golchin, A., Clarke, P., Baldock, J.A., Higashi, T., Skjemstad, J.O., Oades, J.M., 1997b. The effects of vegetation and burning on the chemical composition of soil organic matter in a volcanic ash soil as shown by ^{13}C NMR spectroscopy. I. Whole soil and humic acid fraction. *Geoderma* **76**, 155–174.

Goldberg, E.D., 1985. *Black Carbon in the Environment*. John Wiley & Sons, New York.

Golding, C.J., Smernik, R.J., Birch, G.F., 2004. Characterization of sedimentary organic matter from three south-eastern Australian estuaries using solid-state ^{13}C NMR techniques. *Mar. Fresh. Res.* **55**, 285–293.

Goñi, M.A., Hedges, J.I., 1992. Lignin dimers: Structures, distribution, and potential geochemical applications. *Geochim. Cosmochim. Acta* **56**, 4025–4043.

Goñi, M.A., Nelson, B., Blanchette, R.A., Hedges, J.I., 1993. Fungal degradation of wood lignins: geochemical perspectives from CuO-derived phenolic dimers and monomers. *Geochim. Cosmochim. Acta* **57**, 3985–4002.

Gordon, E.S., Goñi, M.A., 2003. Sources and distribution of terrigenous organic matter delivered by the Atchafalaya River to sediments in the northern Gulf of Mexico. *Geochim. Cosmochim. Acta* **67** (13), 2359–2375.

Hartnett, H.E., Devol, A.H., 2003. Role of a strong oxygen-deficient zone in the preservation and degradation of organic matter: a carbon budget for the continental margins of northwest Mexico and Washington State. *Geochim. Cosmochim. Acta* **67** (2), 247–264.

Hartnett, H.E., Keil, R.G., Hedges, J.I., Devol, A.H., 1998. Influence on oxygen exposure time on organic carbon preservation in continental margin sediments. *Nature* **391**, 372–374.

Hatcher, P.G., Wilson, M.A., 1991. The effect of sample hydration on C-13 CPMAS NMR spectra of fulvic acids. *Org. Geochem.* **17** (3), 293–299.

Hatcher, P.G., Spiker, E.C., Szeverenyi, N.M., Maciel, G.E., 1983. Selective preservation and origin of petroleum-forming aquatic kerogen. *Nature* **305**, 498–501.

Hatcher, P.G., Nanny, M.A., Minard, R.D., Dible, S.D., Carson, D.M., 1995. Comparison of two thermochemolytic methods for the analysis of lignin in decomposing gymnosperm wood: the CuO oxidation method and the method of thermochemolysis with tetramethylammonium hyroxide (TMAH). *Org. Geochem.* **23** (10), 881–888.

Hedges, J.I., Ertel, J.R., 1982. Characterization of lignin by gas capillary chromatography of cupric oxide oxidation products. *Anal. Chem.* **54**, 174–178.

Hedges, J.I., Keil, R.G., 1995. Sedimentary organic matter preservation: an assessment and speculative synthesis. *Mar. Chem.* **49**, 81–115.

Hedges, J.I., Mann, D.C., 1979. The lignin geochemistry of marine sediments from the southern Washington coast. *Geochim. Cosmochim. Acta* **43**, 1809–1818.

Hedges, J.I., Stern, J.H., 1984. Carbon and nitrogen determinations of carbonate-containing solids. *Limnol. Oceanog.* **29** (3), 657–663.

Hedges, J.I., Keil, R.G., Benner, R., 1997. What happens to terrestrial organic matter in the ocean? *Org. Geochem.* **27** (5/6), 195–212.

Hedges, J.I., Hu, F.S., Devol, A.H., Hartnett, H.E., Tsamakis, E., Keil, R.G., 1999. Sedimentary organic matter preservation: a test for selective degradation under oxic conditions. *Am. J. Sci.* **299**, 529–555.

Hedges, J.I., Eglinton, G., Hatcher, P.G., Kirchman, D.L., Arnosti, C., Derenne, S., Evershed, R.P., Kögel-Knabner, I., de Leeuw, J.W., Littke, R., Michaelis, W., Rullkotter, J., 2000a. The molecularly-uncharacterized component (MUC) of nonliving organic matter in natural environments. *Org. Geochem.* **31**, 945–958.

Hedges, J.I., Mayorga, E., Tsamakis, E., McClain, M.E., Aufdenkampe, A., Quay, P., Richey, J.E., Benner, R., Opsahl, S., Black, B., Pimentel, T., Quintanilla, J., Maurice, L., 2000b. Organic matter in Bolivian tributaries of the Amazon River: a comparison to the lower mainstem. *Limnol. Oceanogr.* **45** (7), 1449–1466.

Hedges, J.I., Baldock, J.A., Gélinas, Y., Lee, C., Peterson, M., Wakeham, S.G., 2001. Evidence for non-selective preservation of organic matter in sinking marine particles. *Nature* **409**, 801–804.

Hedges, J.I., Baldock, J.A., Gélinas, Y., Lee, C., Peterson, M.L., Wakeham, S.G., 2002. The biochemical and elemental compositions of marine plankton: a NMR perspective. *Mar. Chem.* **78**, 47–63.

Hwang, J.S., Druffel, E.R.M., 2003. Lipid-like material as the source of the uncharacterized organic carbon in the ocean? *Science* **299** (5608), 881–884.

Keil, R.G., Cowie, G.L., 1999. Organic matter preservation through the oxygen-deficient zone of the NE Arabian Sea as discerned by organic carbon: mineral surface area ratios. *Mar. Geol.* **161** (1), 13–22.

Keil, R.G., Montlucon, D.B., Prahl, F.G., Hedges, J.I., 1994a. Sorptive preservation of labile organic-matter in marine sediments. *Nature* **370** (6490), 549–552.

Keil, R.G., Tsamakis, E., Fuh, C.B., Giddings, J.C., Hedges, J.I., 1994b. Mineralogical and textural controls on the organic composition of coastal marine sediments: Hydrodynamic separation using SPLITT-fractionation. *Geochim. Cosmochim. Acta* **58** (2), 879–893.

Keil, R.G., Mayer, L.M., Quay, P.D., Richey, J.E., Hedges, J.I., 1997. Loss of organic matter from riverine particles in deltas. *Geochim. Cosmochim. Acta* **61** (7), 1507–1511.

Keil, R.G., Tsamakis, E., Giddings, J.C., Hedges, J.I., 1998. Biochemical distributions (amino acids, neutral sugars, and lignin phenols) among size-classes of modern marine sediments. *Geochim. Cosmochim. Acta* **62** (8), 1347–1364.

Keil, R.G., Dickens, A.F., Arnarson, R., Nunn, B.L., Devol, A.H., 2004. What is the oxygen exposure time of laterally transported organic matter along the Washington margin? *Mar. Chem.* **92** (1–4), 157–165.

Kinchesh, P., Powlson, D.S., Randall, E.W., 1995. C-13 NMR studies of organic matter in whole soils. 1. Quantitation Possibilities. *Eur. J. Soil Sci.* **46** (1), 125–137.

Knicker, H., 2000. Biogenic nitrogen in soils as revealed by solid-state carbon-13 and nitrogen-15 nuclear magnetic resonance spectroscopy. *J. Environ. Qual.* **29** (3), 715–723.

Knicker, H., Hatcher, P.G., 1997. Survival of protein in an organic-rich sediment: possible protection by encapsulation in organic matter. *Naturwissenschaften* **84**, 231–234.

Kögel-Knabner, I., 1997. ^{13}C and ^{15}N NMR spectroscopy as a tool in soil organic matter studies. *Geoderma* **80**, 243–270.

Kuhlbusch, T.A.J., 1998. Black carbon and the carbon cycle. *Science* **280**, 1903–1904.

Ludwig, W., Probst, J.L., Kempe, S., 1996. Predicting the oceanic input of organic carbon by continental erosion. *Glob. Biogeochem. Cycles* **10** (1), 23–41.

Masiello, C.A., 2004. New directions in black carbon organic geochemistry. *Mar. Chem.* **92** (1–4), 201–213.

Mayer, L.M., 1994. Relationships between mineral surfaces and organic carbon concentrations in soils and sediments. *Chem. Geol.* **114** (3-4), 347–363.

Minor, E.C., Wakeham, S.G., Lee, C., 2003. Changes in the molecular-level characteristics of sinking marine particles with water column depth. *Geochim. Cosmochim. Acta* **67** (22), 4277–4288.

Nelson, P.N., Baldock, J.A., Clarke, P., Oades, J.M., Churchman, G.J., 1999. Dispersed clay and organic matter in soil: their nature and associations. *Aust. J. Soil Res.* **37**, 289–315.

Newman, R.H., 1992. Nuclear magnetic resonance study of spatial relationships between chemical components in wood cell walls. *Holzforschung* **46** (3), 205–210.

Newman, R.H., Tate, K.R., 1991. C-13 NMR characterization of humic acids from soils of a development sequence. *J. Soil Sci.* **42** (1), 39–46.

Nittrouer, C.A., Sternberg, R.W., 1981. The formation of sedimentary strata in an allochthonous shelf environment: the Washington continental shelf. *Mar. Geol.* **42**, 201–232.

Petsch, S.T., Smernik, R.J., Eglinton, T.I., Oades, J.M., 2001. A solid-state ^{13}C-NMR study of kerogen degradation during black shale weathering. *Geochim. Cosmochim. Acta* **65**, 1867–1882.

Prahl, F.G., Muehlhausen, L.A., Zahnle, D., 1988. Further evaluation of long-chain alkenones as indicators of paleoceanographic conditions. *Geochim. Cosmochim. Acta* **52** (9), 2303–2310.

Prahl, F.G., Ertel, J.R., Goni, M.A., Sparrow, M.A., Eversmeyer, B., 1994. Terrestrial organic-carbon contributions to sediments on the Washington margin. *Geochim. Cosmochim. Acta* **58** (14), 3035–3048.

Preston, C.M., 1996. Applications of NMR to soil organic matter analysis: history and prospects. *Soil Sci.* **161** (3), 144–166.

Preston, C.M., Newman, R.H., 1992. Demonstration of spatial heterogeneity in the organic-matter of de-ashed humin samples by solid-state C-13 CPMAS NMR. *Can. J. Soil Sci.* **72** (1), 13–19.

Preston, C.M., Sollins, P., Sayer, B.G., 1990. Changes in organic-components for fallen logs in old-growth douglas-fir forests monitored by C-13 nuclear magnetic resonance spectroscopy. *Can. J. Forest Res.* **20** (9), 1382–1391.

Ransom, B., Kim, D., Kastner, M., Wainwright, S., 1998. Organic matter preservation on continental slopes: importance of mineralogy and surface area. *Geochim. Cosmochim. Acta* **62** (8), 1329–1345.

Skjemstad, J.O., Taylor, J.A., Smernik, R.J., 1999. Estimation of charcoal (char) in soils. *Commun. Soil Sci. Plant Anal.* **30** (15–16), 2283–2298.

Smernik, R.J., Oades, J.M., 2000a. The use of spin counting for determining quantitation in solid state C-13 NMR spectra of natural organic matter 1. Model systems and the effects of paramagnetic impurities. *Geoderma* **96** (1–2), 101–129.

Smernik, R.J., Oades, J.M., 2000b. The use of spin counting for determining quantitation in solid state C-13 NMR spectra of natural organic matter 2. HF-treated soil fractions. *Geoderma* **96** (3), 159–171.

Smernik, R.J., Oades, J.M., 2001. Solid-state ^{13}C-NMR dipolar dephasing experiments for quantifying protonated and non-protonated carbon in soil organic matter and model systems. *Eur. J. Soil Sci.* **52**, 103–120.

Smernik, R.J., Oades, J.M., 2003. Spin accounting and RESTORE—two new methods to improve quantitation in solid-state C-13 NMR analysis of soil organic matter. *Eur. J. Soil Sci.* **54** (1), 103–116.

Smernik, R.J., Skjemstad, J.O., Oades, J.M., 2000. Virtual fractionation of charcoal from soil organic matter using solid state ^{13}C NMR spectral editing. *Aust. J. Soil Res.* **38**, 665–683.

Smernik, R.J., Baldock, J.A., Oades, J.M., Whittaker, A.K., 2002a. Determination of $T_{1\rho}H$ relaxation rates in charred and uncharred wood and consequences for NMR quantitation. *Solid State Nucl. Mag. Reson.* **22**, 50–70.

Smernik, R.J., Baldock, J.A., Oades, J.M., 2002b. Impact of remote protonation on ^{13}C CPMAS NMR quantitation of charred and uncharred wood. *Solid State Nucl. Mag. Reson.* **22**, 71–82.

Stevenson, F.J., 1994. *Humus Chemistry: Genesis, Composition, Reactions*, second ed. John Wiley & Sons, New York.

Van Andel, T.H., 1964. Recent marine sediments of the Gulf of California. In van Andel, T.H., Shor, G.G. (Eds.), *Marine Geology of the Gulf of California*. American Association of Petroleum Geologists, Memoir No. 3, pp. 216–310.

Wakeham, S.G., Lee, C., Hedges, J., Hernes, P.J., Peterson, M.L., 1997. Molecular indicators of diagenetic status in marine organic matter. *Geochim. Cosmochim. Acta* **61** (24), 5363–5369.

Ward, P.D., Haggart, J.W., Carter, E.S., Wilbur, D., Tipper, H.W., Evans, T., 2001. Sudden productivity collapse associated with the Triassic-Jurassic boundary mass extinction. *Science* **292**, 1148–1151.

Werner-Zwanziger, U., Lis, G., Mastalerz, M., Schimmelmann, A., 2005. Thermal maturity of type II kerogen from the New Albany Shale assessed by ^{13}C CP/MAS NMR. *Solid State Nucl. Magn. Reson.* **27**, 140–148.

White, S., 1970. Mineralogy and geochemistry of continental shelf sediments off the Washington-Oregon coast. *J. Sediment. Petrol.* **40**, 38–54.

Wilson, M.A., 1987. *NMR Techniques and Applications in Geochemistry and Soil Science*. Pergamon Press, NY.

Zumbulyadis, N., 1983. Selective carbon excitation and the detection of spatial heterogeneity in cross-polarization magic-angle spinning NMR. *J. Magnet. Reson.* **53** (3), 486–494.